27. Bis- through Tetrakis-Adducts of C_{60} by Reversible Tether-Directed Remote Functionalization and Systematic Investigation of the Changes in Fullerene Properties as a Function of Degree, Pattern, and Nature of Functionalization

by **Francesca Cardullo, Paul Seiler, Lyle Isaacs, Jean-François Nierengarten, Richard F. Haldimann,** and **François Diederich***

Laboratorium für Organische Chemie, ETH-Zentrum, Universitätstrasse 16, CH-8092 Zürich

Tiziana Mordasini-Denti and **Walter Thiel**

Organisch-chemisches Institut, Universität Zürich, Winterthurerstrasse 190, CH-8057 Zürich

and **Corinne Boudon, Jean-Paul Gisselbrecht,** and **Maurice Gross**

Laboratoire d'Electrochimie et de Chimie Physique du Corps Solide, U.R.A. au C.N.R.S. n° 405, Faculté de Chimie, Université Louis Pasteur, 1 et 4, rue Blaise Pascal, F-67008 Strasbourg Cedex

(4.XII.96)

By the tether-directed remote functionalization method, a series of bis- to hexakis-adducts of C_{60}, *i.e.*, **1**–**7** (*Fig. 1*), had previously been prepared with high regioselectivity. An efficient method for the removal of the tether-reactive-group conjugate was now developed and its utility demonstrated in the regioselective synthesis of bis- to tetrakis(methano)fullerenes (= di- to tetracyclopropafullerenes-C_{60}-I_h) **9**–**11** starting from **4**, **5**, and **7**, respectively (*Schemes 2, 4,* and *5*). This versatile protocol consists of a $^1O_2$ ene reaction with the two cyclohexene rings in the starting materials, reduction of the formed mixture of isomeric allylic hydroperoxides to the corresponding alcohols, acid-promoted elimination of H_2O to cyclohexa-1,3-dienes, *Diels-Alder* addition of dimethyl acetylenedicarboxylate, *retro-Diels-Alder* addition, and, ultimately, transesterification. In the series **9**–**11**, all methano moieties are attached along an equatorial belt of the fullerene. Starting from C_{2v}-symmetrical tetrakis-adduct **15**, transesterification with dodecan-1-ol or octan-1-ol yielded the octaesters **16** and **17**, respectively, as noncrystalline fullerene derivatives (*Scheme 3*). The X-ray crystal structure of a $CHCl_3$ solvate of **11** (*Fig. 3*) showed that the residual conjugated π-chromophore of the C-sphere is reduced to two tetrabenzopyracylene substructures connected by four biphenyl-type bonds (*Fig. 5*). In the eight six-membered rings surrounding the two pyracylene (= cyclopent[*fg*]acenaphthylene) moieties, 6-6 and 6-5 bond-length alteration (0.05 Å) was reduced by *ca.* 0.01 Å as compared to the free C_{60} skeleton (0.06 Å) (*Fig. 4*). The crystal packing (*Fig. 6*) revealed short contacts between Cl-atoms of the solvent molecule and sp^2- and sp^3-C-atoms of the C-sphere, as well as short contacts between Cl-atoms and O-atoms of the EtOOC groups attached to the methano moieties of **11**. The physical properties and chemical reactivity of compounds **1**–**11** were comprehensively investigated as a function of degree and pattern of addition and the nature of the addends. Methods applied to this study were UV/VIS (*Figs. 7–11*), IR, and NMR spectroscopy (*Table 2*), cyclic (CV) and steady-state (SSV) voltammetry (*Table 1*), calculations of the energies of the *l*owest *u*noccupied *m*olecular *o*rbitals (LUMOs) and electron affinities (*Figs. 12* and *13*), and evaluation of chemical reactivity in competition experiments. It was found that the properties of the fullerene derivatives were not only affected by the degree and pattern of addition but also, in a remarkable way, by the nature of the addends (methano *vs.* but-2-ene-1,4-diyl) anellated to the C-sphere. Attachment of multiple methano moieties along an equatorial belt as in the series **8**–**11** induces only a small perturbation of the original fullerene π-chromophore. In general, with increasing attenuation of the conjugated fullerene π-chromophore, the optical (HOMO-LUMO) gap in the UV/VIS spectrum is shifted to higher energy, the number of reversible one-electron reductions decreases, and the first reduction potential becomes increasingly negative, the computed LUMO energy increases and the electron affinity decreases, and the reactivity of the fullerene towards nucleophiles and carbenes and as dienophile in cycloadditions decreases.

1. Introduction. – In the preceding paper [1], we described a versatile, tether-directed remote functionalization method by which a complete series of bis- to hexakis-adducts of C_{60} such as **1**–**7** (*Fig. 1*) was prepared with high regioselectivity [2] [3]. Hexakis-adduct **7** is characterized by a pseudo-octahedral functionalization pattern, and the addends in the lower adducts partially occupy the sites determined by this pattern. We subsequently became interested in expanding the scope of this methodology by developing a protocol to remove the initially introduced tether-reactive-group conjugate [4]. By this *reversible* tether-directed remote functionalization strategy (*Scheme 1*), the anchor-tether-reactive

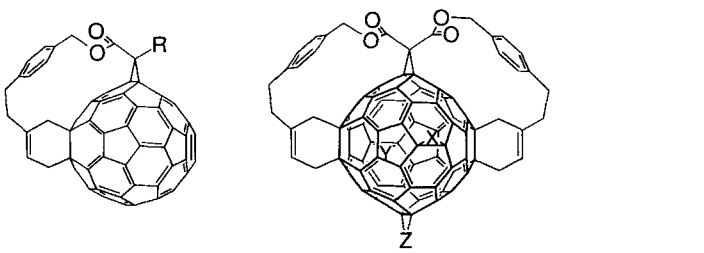

1 R = H
2 R = COOMe

3 X = Y = Z = ——
4 X = $(EtO_2C)_2C$, Y = Z = ——
5 X = Z = $(EtO_2CCH_2O_2C)_2C$, Y = ——
6 X = Y = $(EtO_2CCH_2O_2C)_2C$, Z = ——
7 X = Y = Z = $(EtO_2C)_2C$

Fig. 1. *Bis- to hexakis-adducts* **1**–**7** *obtained by tether-directed remote functionalization*

Scheme 1. *Reversible Tether-Directed Remote Functionalization*

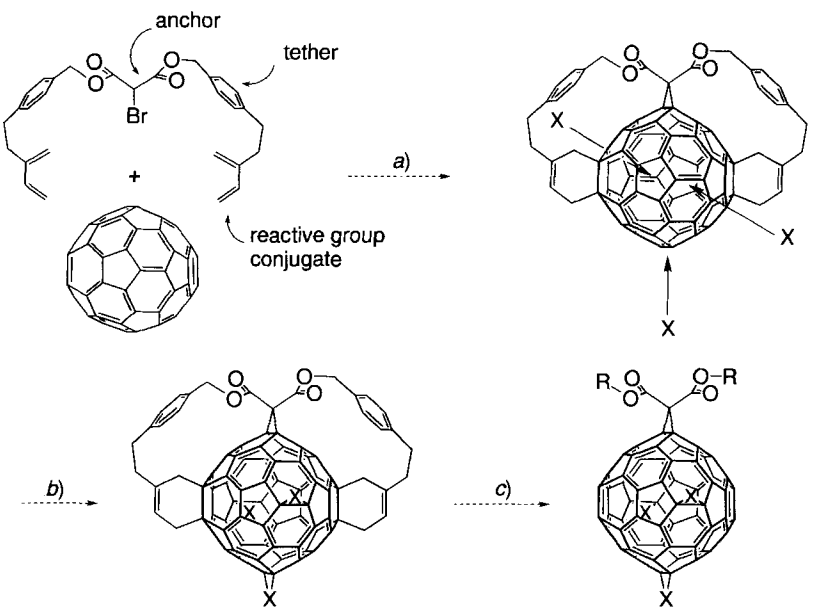

a) The anchor-tether-reactive-group conjugate is introduced. *b*) The anchor-tether-reactive group directs newly incoming addends into equatorial positions. *c*) Subsequently, the tether-reactive-group conjugate is removed.

group conjugate would first be attached to C_{60} and then direct new incoming addends with high regioselectivity into equatorial (*e*) positions [2b] [5]. Subsequent removal of the tether-reactive-group conjugate would yield new multiple adducts with addition patterns that are difficult or even impossible to be accessed by stepwise additions without tether or template assistance.

In this paper, we report an efficient method for the removal of the tether-reactive group conjugate and demonstrate its utility by the synthesis of bis- to tetrakis(methano)fullerenes (= di- to tetracyclopropafullerenes-C_{60}-I_h) **9**–**11** (*Fig. 2*). These compounds are members of a series of adducts (**8a**/**b** [6] and **9**–**11**) in which methano moieties are progressively introduced along an equatorial belt of the C-sphere. The X-ray crystal-structure analysis of tetrakis-adduct **11** is also described. Previously, **9** had been obtained as the kinetically most favorable constitutional isomer by stepwise *Bingel* cyclopropanation [6a] of C_{60}, followed by HPLC separation from the other six regioisomeric bis-adducts formed [5]. Tris-adduct **10** and tetrakis-adduct **11** cannot be prepared without tether or template assistance; addition of a third and forth addend to **9** and **10**, respectively, would occur at the 6-6 bond (bond at the junction between two six-membered rings) which is equatorial to all addends already in place (*Fig. 2*) [2] [5] [7].

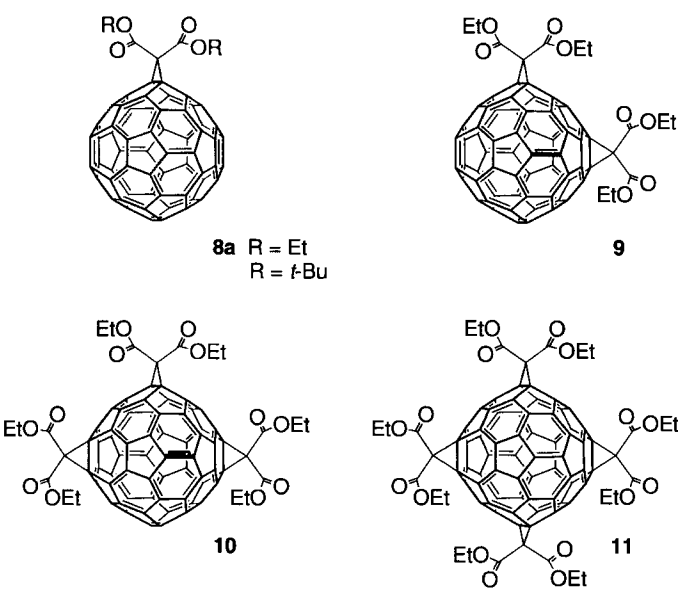

Fig. 2. *Bis- to tetrakis(methano)fullerenes* **9**–**11** *obtained by reversible tether-directed remote functionalization.* In **8**–**11**, addends are progressively introduced along an equatorial belt of the C-sphere. The 6-6 bonds in **9** and **10** that react preferentially with untethered nucleophiles are highlighted in bold.

This paper not only highlights the power of tethered synthesis in the regioselective formation of fullerene multiple adducts [1–4] [8–10], but also contains an in-depth analysis of the changes in chemical reactivity and physical properties that occur when the conjugated fullerene π-chromophore is reduced in a specific way as a result of increasing functionalization. In addition, the dependence of fullerene properties from the nature of the addends anellated to the C-sphere is investigated.

2. Results and Discussion. – 2.1. *Synthesis of Tetrakis(methano)fullerenes. Diels-Alder* adducts of fullerenes [11] with buta-1,3-diene derivatives [12] have proven quite stable towards *retro-Diels-Alder* reaction. Therefore, an elegant, although less direct procedure, introduced by *Rubin* and coworkers [13a], was applied to the removal of the two cyclohexene rings in hexakis-adduct **7**. When a solution of **7** [1] in PhCl was irradiated in the presence of C_{60} as $^1O_2$ photosensitizer [14] at 20° with a medium-pressure Hg lamp (*Pyrex* filter) while a stream of O_2 was bubbled through, the $^1O_2$ ene reaction (the *Schenck* reaction) [15] at the two cyclohexene rings was completed within 2 h yielding a mixture of isomeric allylic hydroperoxides **12** (*Scheme 2*). *In situ* reduction of **12** with PPh_3 gave a mixture of isomeric allylic alcohols **13** in 90% yield. Matrix-assisted laser-desorption-ionization time-of-flight (MALDI-TOF) mass spectrometry confirmed the formation of diols **13** by showing the molecular ion as the base peak at *m/z* 1669. When the $^1O_2$ ene reaction of **7** was repeated in the absence of C_{60}, the yield of **13**, after reduction, was only 42%. This demonstrates that hexakis-adduct **7**, in contrast to the parent fullerene and lower adducts [1] [14c], had lost much of its capacity for acting as $^1O_2$ photosensitizer.

By the $^1O_2$ ene reaction of **7** and subsequent reduction, three constitutionally isomeric allylic alcohols with endocyclic double bonds could form [13b]. Three major product fractions were detectable (TLC), and the least polar one was isolated by column chromatography (SiO_2-*H*, CH_2Cl_2/AcOEt 23:2). Its ^{1}H-NMR spectrum ($CDCl_3$) gave evidence for the presence of constitutional isomer **13** (depicted in *Scheme 2*) in which both $CH_2C_6H_4C_2H_4$ tethers are attached to the cyclohexene C-atoms bearing the OH groups.

Scheme 2. *Synthesis of* D_{2h}*-Symmetrical Tetrakis(methano)fullerene* **11**

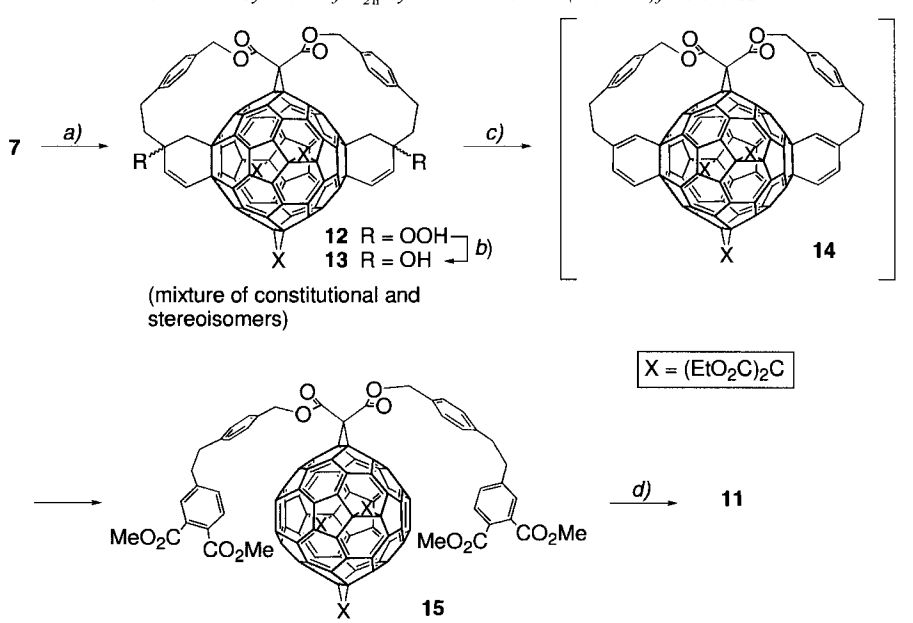

a) *hv* (medium pressure Hg lamp, *Pyrex* filter), O_2, C_{60}, PhCl, 2 h. *b*) PPh_3, PhCl, 1 h; 90% (from **7**). *c*) $MeO_2CC{\equiv}CCO_2Me$ (10 equiv.), TsOH (3 equiv.), PhMe, *Δ*, 4.5 h; 47%. *d*) K_2CO_3, EtOH, THF, 3.5 h; 80%.

The ^{1}H-NMR spectrum of **13** displayed two *d*'s (J = 9.8 Hz) at 6.17 and 6.26 ppm for the coupled vinylic protons of the cyclohexene moieties. Furthermore, four *d*'s (J = 11 Hz) for the diastereotopic $C_6H_4CH_2O$ protons suggested the presence of two, C_s(*meso*) and C_2(*rac*) symmetrical diastereoisomers. A total of at least 54 signals in the sp^2-C-atom region (128–157 ppm) of the ^{13}C-NMR spectrum also supported the presence of the two diasteroisomers which require 30 signals each in this region.

The mixture of allylic alcohols **13** was subsequently heated in deoxygenated PhMe in the dark together with toluene-4-sulfonic acid (TsOH, 3 equiv.) and dimethyl acetylenedicarboxylate (DMAD, 10 equiv.). Under these conditions, **13** was dehydrated to the corresponding bis(cyclohexa-1,3-diene) derivative **14** which, *via* a *Diels-Alder/retro-Diels-Alder* sequence, afforded tetrakis-adduct **15** in 42% overall yield starting from **7**.

The MALDI-TOF mass spectrum of **15** showed the expected molecular ion as the base peak at *m/z* 1916. In support of the proposed C_{2v}-symmetrical structure, the ^{1}H-NMR spectrum ($CDCl_3$) of **15** displayed resonances for three chemically nonequivalent EtO groups. The ^{13}C-NMR spectrum ($CDCl_3$) exhibited 16 of the 17 expected resonances for fullerene C-atoms and displayed signals for three nonequivalent EtOOC groups.

Various transesterification methods were explored to convert **15** into the D_{2h}-symmetrical target compound **11**. Heating **15** in EtOH/CH_2Cl_2 for 1 d to reflux in the presence of tetraethyl titanate [16] as catalyst only led to the recovery of starting material. Presumably, the titanate reagent is too sterically hindered to catalyze reactions in close proximity of the bulky fullerene sphere. Finally, treatment of **15** with a large excess of K_2CO_3 in anhydrous EtOH/THF 1:1 [8] [9] for 3.5 h yielded the desired octakis(ethyl ester) **11** as a bronze-colored solid. Both **11** and **15** give green-yellow solutions in CH_2Cl_2 (for the UV/VIS spectra, see *Sec. 2.6.2*).

The LDI-TOF mass spectrum of **11** displayed the expected molecular ion as the base peak at *m/z* 1353. In support of the D_{2h}-symmetrical structure, the ^{1}H-NMR spectrum ($CDCl_3$) showed only peaks for two chemically nonequivalent EtO groups. Also, the ^{13}C-NMR spectrum ($CDCl_3$) of **11** depicted only seven resonances (one of half intensity) for fullerene sp^2-C-atoms, two signals for fullerene sp^3-C-atoms, two for methano-moiety C-atoms, and the expected peaks for two nonequivalent EtOOC groups.

2.2. *X-Ray Crystal Structure of Tetrakis-adduct* **11**. Black, plate-like single crystals of **11** were obtained by very slow evaporation of a $CHCl_3$ solution at room temperature. The crystals belong to the triclinic space group $P\bar{1}$, with half a molecule of **11** and one $CHCl_3$ molecule in the asymmetric unit. The structure of **11** undergoes a phase transformation at *ca.* 252 K, the low-temperature phase being triclinic ($P\bar{1}$) as well. The high- and low-temperature structures of **11** were determined at 258 and 100 K, respectively. In the high-temperature structure, the solvent and two EtO groups are statically disordered, while the low-temperature structure is ordered. Further details about the X-ray analysis are given in the *Exper. Part.*

The four addition sites containing the diethyl malonate addends for the low-temperature structure are shown in *Fig. 3*. According to the ^{1}H- and ^{13}C-NMR spectra, the average symmetry of **11** in solution is D_{2h}, while the crystal structure is centrosymmetric with two pairs of symmetry-related fusion bonds (bonds between two bridgehead C-atoms). The degree of deformation within the four methano-bridged pyracylenes is very similar to that observed for such subunits in two hexakis-adducts of C_{60} [10a] [17]. The C_{60} skeleton itself has a pseudo-ellipsoidal shape, with principal axes of *ca.* 7.37, 7.31, and 6.88 Å, the shortest axis being perpendicular to the equatorial plane containing

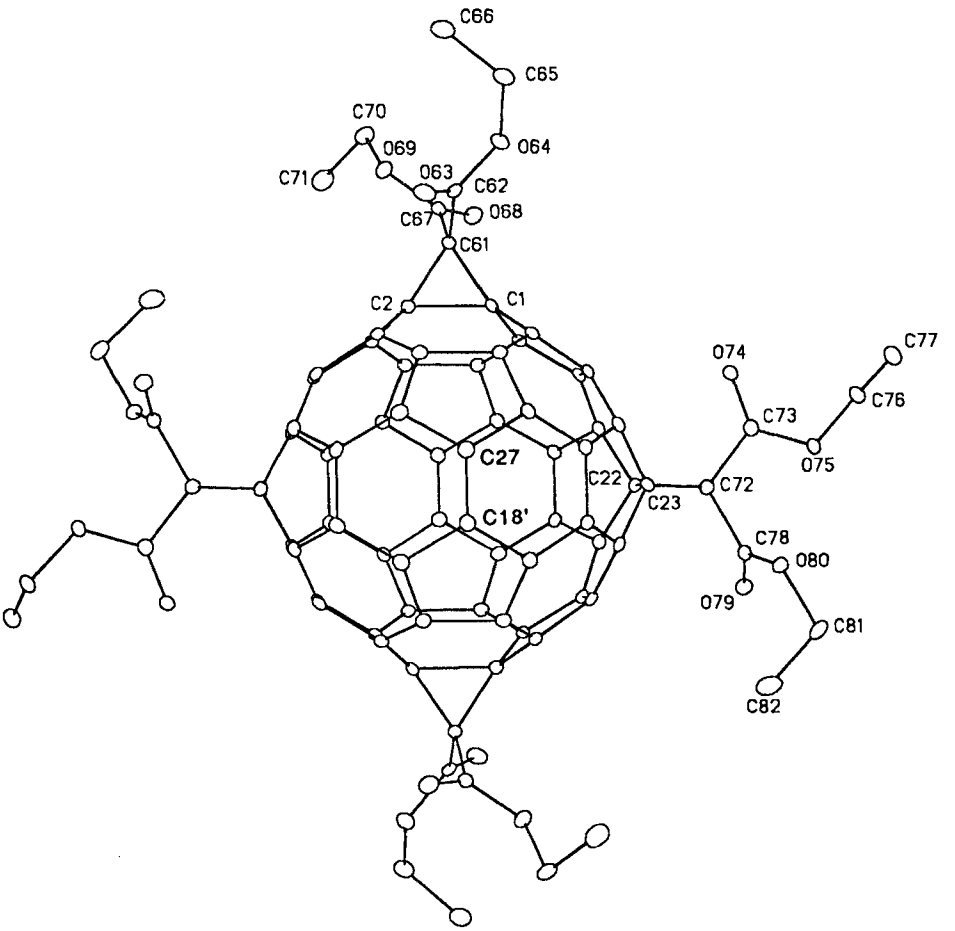

Fig. 3. *Low-temperature crystal structure of* **11**. Vibrational ellipsoids obtained at 100 K are drawn at the 30% probability level.

the four methano moieties. A striking feature in the present structure is the difference between the (symmetry-inequivalent) fusion-bond lengths C(1)–C(2) of 1.614(4) Å and C(22)–C(23) of 1.577(5) Å (*Fig. 4*). The difference between these C–C single-bond lengths may be connected with the actual shape of the C_{60} spheroid, since the longest axis is parallel to the (longer) C(1)–C(2) bond, and the shortest axis is parallel to the (shorter) C(22)–C(23) bond. A similar trend occurs in a C_{60} hexakis-adduct [17].

The residual conjugated π-electron chromophore in **11** consists of two formal tetrabenzopyracylene substructures connected by four biphenyl-type bonds (*Fig. 5*; pyracylene = cyclopent[*fg*]acenaphthylene). The functionalization of the C_{60} sphere hardly affects the length of the central 6-6 bond C(18')–C(27) in the tetrabenzopyracylene moiety; its value (1.387(4) Å) (*Fig. 4*) is not significantly shorter than the mean 6-6 bond length (1.391 Å) derived in two (nearly regular) C_{60} hemispheres [8] [19], in other words, there is no structural evidence for an enhanced reactivity (see *Sect. 2.6.6* below) of this

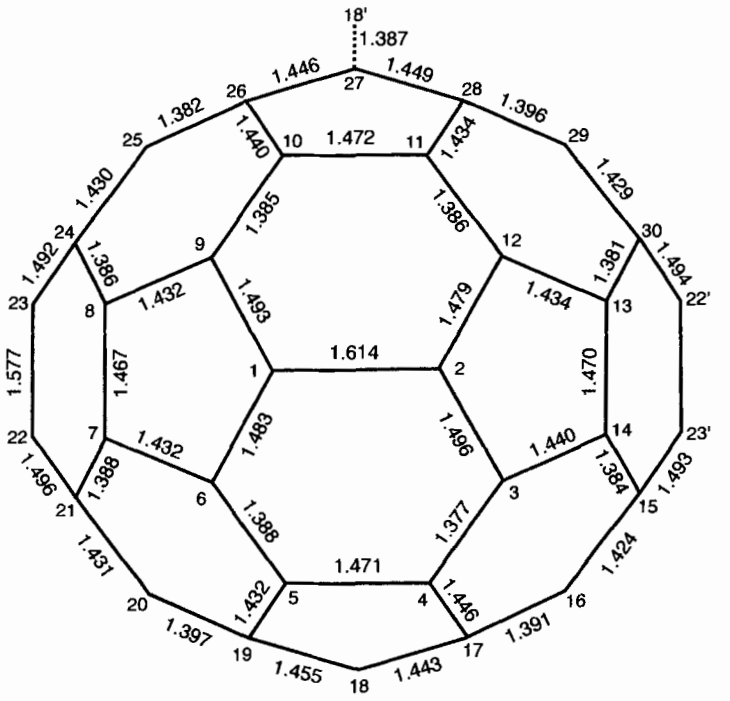

Fig. 4. *Fullerene hemisphere of* **11** *in a view on the cyclopropane-fused equatorial belt including symmetry-independent bond lengths.* Estimated standard deviations are *ca.* 0.005 Å.

bond. The molecular geometry of the two tetrabenzopyracylene substructures has also been analyzed. It appears that the bond-length alteration (of shorter 6-6 and longer 6-5 bonds, see *Fig. 4*) within the eight six-membered rings, fused to the two central pyracylene substructures (*Fig. 5*), is reduced slightly with respect to the free C_{60} skeleton from *ca.* 0.06 to *ca.* 0.05 Å.

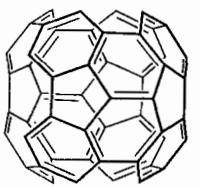

Fig. 5. *Schematic illustration of the conjugated π-chromophore in tetrakis-adduct* **11** *composed of two tetrabenzopyracyclene substructures connected by four biphenyl-type bonds*

In the disordered high-temperature structure of **11**, an estimation of intermolecular contacts is problematic. Nevertheless, preliminary results indicate that no short intermolecular contacts occur among neighboring fullerenes, or among solvent and fullerene molecules, in contrast to the low-temperature structure, in which the ordered solvent is in contact with three neighboring fullerenes. *Fig. 6* shows that Cl(1) makes two short contacts with **11**(a), namely with the carbonyl O(79) of an EtO_2C group (3.17 Å), and

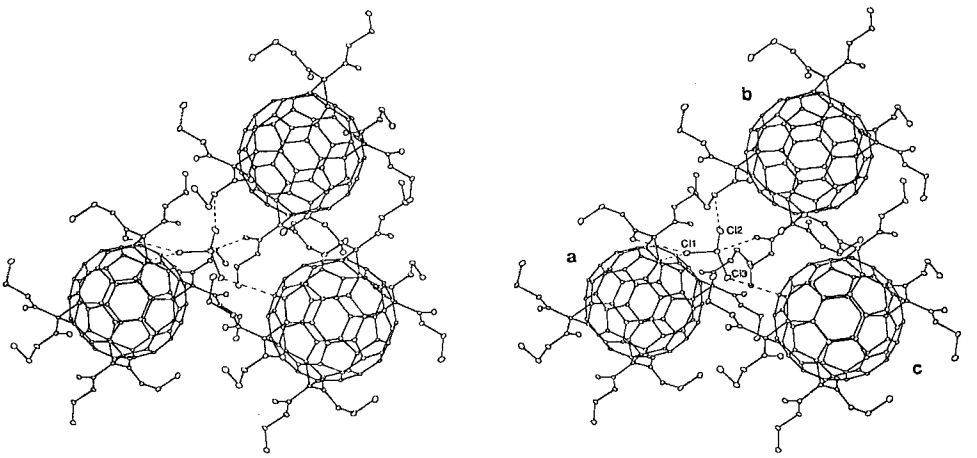

Fig. 6. *Short intermolecular contacts between three molecules of* **11** *and a* $CHCl_3$ *molecule at 100 K*

with the bridgehead atom C(22) (3.32 Å). Cl(2) is in contact with the ethoxy O-atom O(64) of **11**(b) (3.04 Å), and Cl(3) is in contact with C(4) (3.31 Å) of the C_{60} core of **11**(c); the C-atom of the solvent makes one short contact to the carbonyl O(74) of **11**(b) (3.14 Å). It seems plausible that the ordering process of solvent and diethyl malonate addends (and the resulting stabilization of the crystal structure) is the driving force for the phase transition observed at *ca.* 252 K.

2.3. *Preparation of Tetrakis(methano)fullerenes with Long-Chain Alkyl Esters.* As part of our program in new fullerene-based materials [8] [18], we became interested in preparing noncrystalline [20] and, ultimately, liquid-crystalline [21] derivatives. Therefore, we intended to prepare D_{2h}-symmetrical analogs of **11** with eight long-chain alkyl esters attached to the four methano moieties.

When the transesterification of **15** with dodecan-1-ol was attempted under the conditions which yielded octakis(ethyl ester) **11** (K_2CO_3, dodecan-1-ol (800 equiv.), THF), only starting material was recovered after 5 h. Similarly, the use of a larger excess of dodecan-1-ol (> 4000 equiv.) and addition of [18]crown-6 (4 equiv.) to increase the solubility of K_2CO_3 in the dodecan-1-ol/THF mixture did not yield any product after 3 h. Stirring overnight, after adding a large excess of [18]crown-6 (40 equiv.), induced a color change from yellow-green to dark-green, but TLC (SiO_2, CH_2Cl_2/MeOH 1:1) indicated mainly conversion to baseline material. However, when Cs_2CO_3 was used as a more soluble base, formation of several apolar products was observed, and conversion of **15** was completed within 1 d, after which the desired octaester **16** was isolated in 14% yield after prep. HPLC (SiO_2, CH_2Cl_2/hexane 1:1) (*Scheme 3*). Compound **17** was prepared under similar conditions using octan-1-ol as the alcohol, and prep. HPLC (SiO_2, CH_2Cl_2/hexane 3:2) yielded the pure octaester in 16% yield. Prep. HPLC was required for complete purification of both **16** and **17** due to the difficult separation of the desired products from a slightly faster eluting major by-product resulting from mono-decarboxylation. The presence of this by-product, in which one of the ROOC residues in **16** and **17** is replaced by a H-atom, was confirmed by ^{1}H- and ^{13}C-NMR ($CDCl_3$) and, in particular, by fast-atom-bombardment (FAB) mass spectrometry. The mass spectra of

Scheme 3. *Synthesis of* D_{2h}*-Symmetrical Tetrakis(methano)fullerenes* **16** *and* **17**

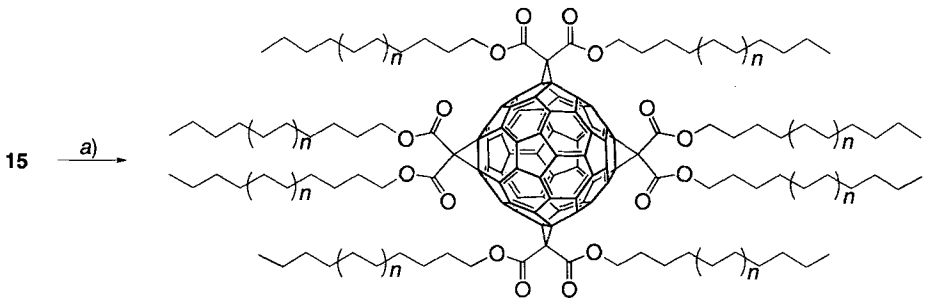

16 $n = 2$ (14%)
17 $n = 0$ (16%)

a) Cs_2CO_3, THF, dodecan-1-ol, 24 h (**16**) or octan-1-ol, 6 h (**17**).

the mono-decarboxylated products showed the molecular ions as base peaks at *m/z* 2262 (by-product of **16**) and *m/z* 1869 (by-product of **17**). Hydrolysis followed by decarboxylation [8] becomes competitive with the transesterification reaction, when the used base and the solvents are not completely dry and when prolonged reaction times are required.

The spectral properties of both long-chain esters **16** and **17** were expectedly quite similar. The FAB mass spectra of **16** and **17** showed the molecular ions as the base peaks at *m/z* 2475 ($\mathbf{16}^+$) and 2026 ($\mathbf{17}^+$), respectively, accompanied by a major fragment resulting from loss of an alkyloxy residue. With the exception of the alkyl ester resonances, the ^{13}C-NMR spectra ($CDCl_3$) of **16** and **17** closely resembled that of octakis-(ethyl ester) **11** with identical symmetry. They both formed yellow-brownish, highly viscous oils at room temperature.

2.4. *Synthesis of Bis(methano)fullerene* **9**. The preparation of **9** (*Scheme 4*) was carried out starting from the C_s-symmetrical tetrakis-adduct **4** [1] and followed the protocol which yielded tetrakis(methano)fullerene **11** (*Sect. 2.1*). The $^1O_2$ ene reaction to **18** and subsequent reduction afforded the mixture of allylic alcohols **19** which was characterized by MALDI-TOF mass spectrometry (*m/z* 1353 (100, M^+)). Treatment of **19** with TsOH and DMAD yielded, after column chromatography, C_s-symmetrical bis-adduct **20** (20% yield) as a brown solid which dissolves in CH_2Cl_2 to give red-brown solutions. The low yield was due to the tedious purification from traces of two unidentified by-products which gave red and orange solutions in CH_2Cl_2. Transesterification (K_2CO_3, EtOH/THF 1:1) ultimately afforded the desired C_s-symmetrical *e*-bis-adduct **9**.

The C_s-symmetrical structure of **20** (MALDI-TOF-MS: *m/z* 1601 (100, M^-)) was supported in the ^{13}C-NMR spectrum ($CDCl_3$) by the presence of resonances for two chemically nonequivalent EtOOC groups, two *d*'s for the diastereotopic $C_6H_4CH_2O$ protons, and the appearance of all 32 resonances expected for fullerene C-atoms. Tetrakis-(ethyl ester) **9** showed all spectra in agreement with those reported previously [5].

2.5. *Synthesis of Tris(methano)fullerene* **10**. In analogy to the preparation of **9** and **11**, tris-adduct **10** was obtained starting from pentakis-adduct **5** [1] *via* the sequence **21** → **22** → **23** → **10** (*Scheme 5*). Change of the solution color from orange (**5**, **21**, and **22**) to red-brown (**23**) was a first indication of tris-adduct formation. The ^{13}C-NMR spec-

Scheme 4. *Synthesis of* C_s*-Symmetrical Bis(methano)fullerene* **9**

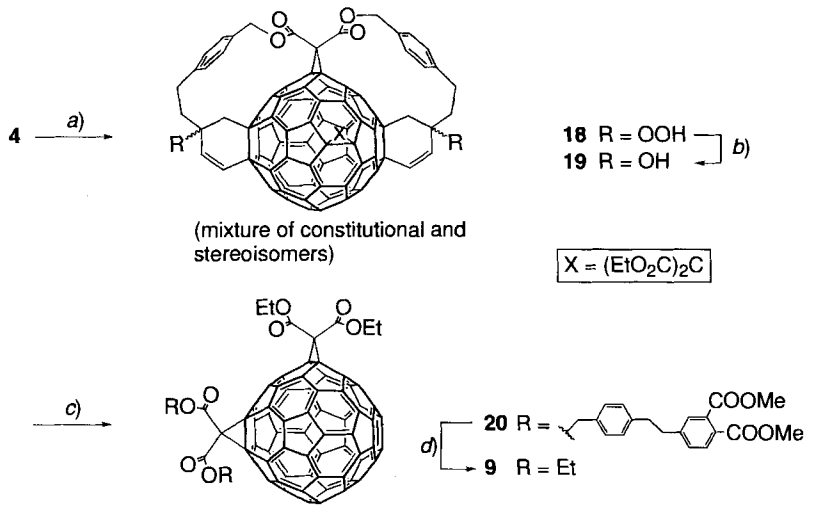

a) *hv*, O_2, C_{60}, PhCl, 2 h. *b*) PPh_3, PhCl, 1 h, 72% (from **4**). *c*) $MeO_2CC{\equiv}CCO_2Me$ (10 equiv.), TsOH (3 equiv.), PhMe, Δ, 4.5 h; 20%. *d*) K_2CO_3, EtOH, THF, 4.5 h; 77%.

Scheme 5. *Synthesis of* C_{2v}*-Symmetrical Tris(methano)fullerene* **10**

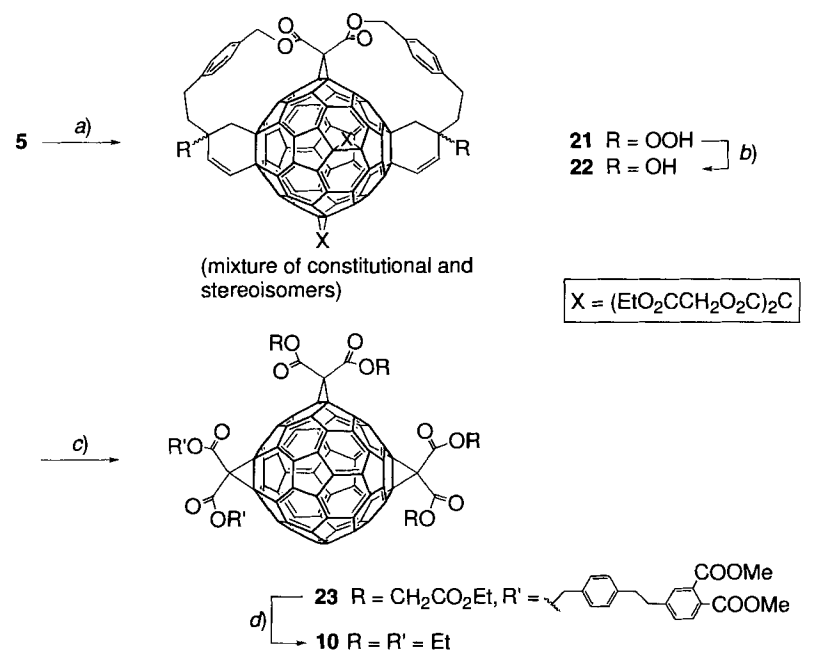

a) *hv*, O_2, C_{60}, PhCl, 2 h. *b*) PPh_3, PhCl, 3 h, 86% (from **5**). *c*) $MeO_2CC{\equiv}CCO_2Me$ (10 equiv.), TsOH (3 equiv.), PhMe, Δ, 5 h; 48%. *d*) K_2CO_3, EtOH, THF, 1.5 h; 83%.

trum ($CDCl_3$) of **23** (MALDI-TOF-MS: *m/z* 1991 (100, M^-)) confirmed the C_s-symmetrical structure by exhibiting 31 of the 32 expected resonances for fullerene C-atoms and signals for three nonequivalent $EtO_2CCH_2O_2C$ groups. The C_{2v}-symmetrical structure of the novel tris-adduct **10** (FAB-MS: *m/z* 1195 (100, MH^+)) was supported by its ^{1}H-NMR spectrum ($CDCl_3$) which displayed two sets of resonances for EtO groups. The ^{13}C-NMR spectrum ($CDCl_3$) displayed all 14 resonances expected for fullerene sp^2-C-atoms (one of half intensity), three signals for fullerene sp^3-C-atoms, two for methano C-atoms (one of half intensity), and the expected peaks for two nonequivalent EtOOC groups.

2.6. *Analysis of the Changes in Properties of Fullerene Derivatives as a Function of Degree and Pattern of Addition and the Nature of the Bridging Addends.* 2.6.1. *Preliminary Remarks.* With compounds **1**–**11** as well as **15**, **20**, and **23**, a unique series of multiple adducts of C_{60} was available for a detailed investigation of the changes in physical properties and chemical reactivity that occur as a function of degree and pattern of addition and the nature of the fused addends.

2.6.2. *Electronic-Absorption Spectroscopy.* A comparison of the UV/VIS spectra of the various C_{60} multiple adducts in CH_2Cl_2 showed four general trends.

i) Changes in the extension of the conjugated π-chromophore of the fullerene have a pronounced effect on spectral shape and the position of the end absorption (the optical gap). This is illustrated in *Fig. 7* by the comparison of the spectra of C_{60}, mono-adduct **8b**, bis-adduct **1**, tris-adduct **3**, tetrakis-adduct **4**, and hexakis-adduct **7**. C_{60} itself gives a purple solution as a result of the broad absorption between 475 and 650 nm. Methanofullerene **8b** [6b] displays two distinct absorption bands at λ_{max} 427 and 489 nm which are characteristic of all C_{60} mono-adducts [11a] [12a] [22], but whose origin is not

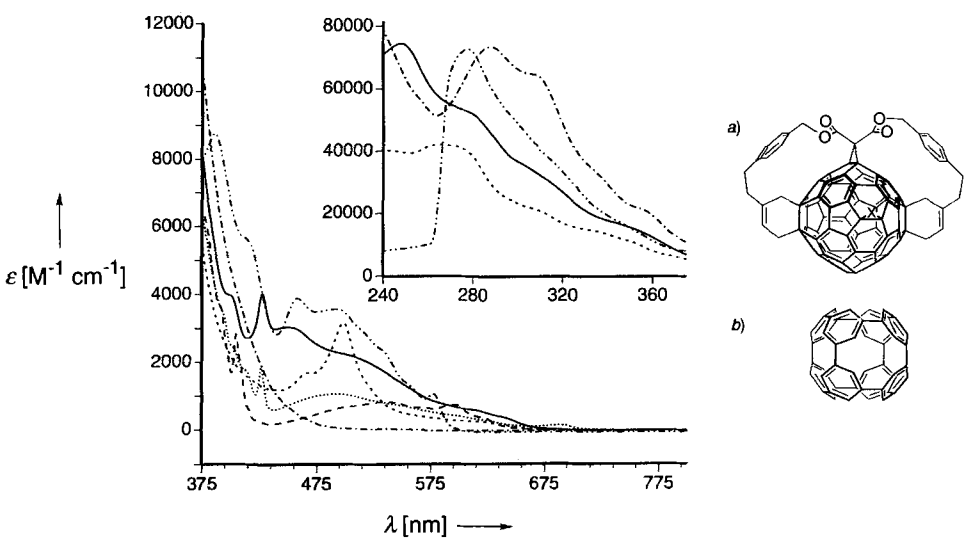

Fig. 7. *UV/VIS Spectra in CH_2Cl_2 of C_{60}* (----), *mono-adduct* **8b** (·····), *bis-adduct* **1** (——), *tris-adduct* **3** (- - -), *tetrakis-adduct* **4** (— · · —), *and hexakis-adduct* **7** (— · — · —). Also shown are *a*) the two benzenoid rings contained in the chromophore of **4** and *b*) a schematic illustration of the benzenoid 'cubic' cyclophane substructure in **7**.

understood. The broad absorption band in the VIS seen in the spectrum of C_{60} is generally less structured and hypsochromically shifted in the spectra of mono-adducts; for **8**, the maximum was observed around 500 nm. The spectrum of bis-adduct **1**, which gives orange-brown solutions, resembles in its general shape the spectrum of a mono-adduct, although the broad VIS absorption band displays both a hyperchromic and a hypsochromic shift (to λ_{max} 449 nm). In a characteristic manner, the diagnostic mono-adduct peak around 700 nm is no longer observed for bis-adduct **1**, whereas the second peak at λ_{max} 427 nm is maintained in the spectrum.

Tris-adduct **3** is orange-brown in concentrated solution and visually indistinguishable from bis-adduct **1**. However, the UV/VIS spectra of the two compounds are quite different. The spectrum of **3** exhibits little fine structure, and the characteristic band around 430 nm, which is present in the spectra of mono- and bis-adducts, is no longer observed. The spectrum is dominated by a broad, relatively intense band at λ_{max} 498 nm. Tetrakis-adduct **4** has a red color in solution, and absorptions in both UV and VIS ranges are much more intense than those of tris-adduct **3**. Compared to the lower adducts **1** and **3**, the end absorption in the spectrum of **4** appears at significantly lower wavelength below 600 nm. This can be explained by the specific functionalization pattern in **4** which generates two benzenoid rings with rather localized electronic sextets (*Fig. 7*) and, correspondingly, reduces the size of the delocalized fullerene π-chromophore. Hexakis-adduct **7** is bright-yellow in the crystalline state and in solution, and, accordingly, its UV/VIS spectrum only exhibits minimal absorption in the VIS region, tailing until λ 460 nm. This drastic blue-shift of the end absorption of **7** is in full accord with the reduced conjugation in the residual π-chromophore consisting of eight formally benzenoid rings arranged in a 'cubic' cyclophane structure (*Fig. 7*). Bond-length alteration typically observed for C_{60} and lower adducts (6-6 bonds *ca.* 0.06 Å shorter than 6-5 bonds) is significantly reduced (by *ca.* 0.02 to 0.03 Å) in the eight aromatic rings of this chromophore [2b] [10a] [17] [23].

It becomes clear from this study that the addition-mediated generation of isolated benzenoid rings within the residual fullerene π-chromophore induces a particularly large hypsochromic shift of the end absorption.

ii) The nature of the addition pattern determines the electronic absorption properties of regioisomeric higher adducts. The specific location of the sites of multiple additions affects the extension and character (benzenoid/non-benzenoid) of the residual fullerene π-chromophore and, therefore, influences the UV/VIS spectrum. *Hirsch et al.* [5] [24] [25a] and, later, *Wilson* and coworkers [25b] showed that the spectra of regioisomeric bis(methano)fullerenes differed distinctively from one another. Such spectral differences also exist between isomeric higher adducts as we observed for the two pentakis-adducts **5** and **6** (*Fig. 8*). The colors of both compounds in solution differ significantly; whereas **5** is orange-red, compound **6** is pale-orange. Accordingly, their UV/VIS spectra are quite different and the end absorption of **5** (590 nm) is significantly red-shifted as compared to that of **6** (550 nm). Interestingly, the spectra of pentakis-adduct **5** and tetrakis-adduct **4**, both with C_s symmetry, exhibit not only similar optical gaps but also similar shape and structure in the VIS region between 400 and 600 nm (*Fig. 8*), which accounts for the similarity in the colors observed in solution. This similarity between the UV/VIS spectra of **4** and **5** correlates with their chemical reactivity toward nucleophiles (*Sect. 2.6.6*) and their propensity to undergo electrochemical reduction (*Sect. 2.6.3*).

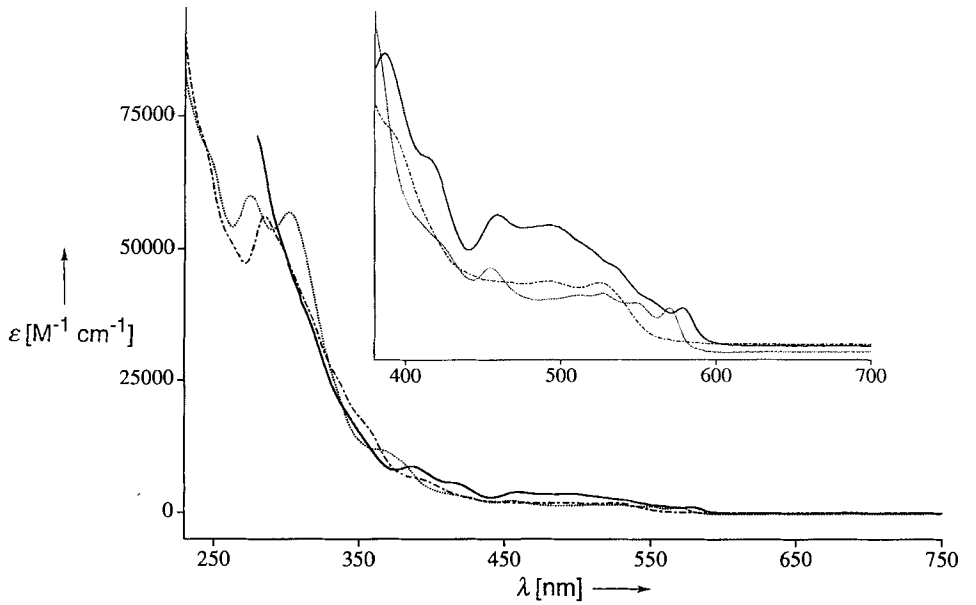

Fig. 8. *UV/VIS Spectra in CH_2Cl_2 of pentakis-adducts* **5** (·····) *and* **6** (– · – · –) *in comparison to* **4** (——)

iii) The nature of the fused addends strongly influences the UV/VIS spectra of fullerene multiple adducts. Remarkable differences in absorption band position and shape were observed for compounds with identical addition patterns but with different fused addends (cyclopropane *vs.* cyclohexene fusion). This is shown in *Figs. 9* and *10* for comparisons between bis- and tris-adducts. The spectrum of the red-brown bis(methano) derivative **9** (*Fig. 9*) resembles more closely the spectrum of fullerene mono-adducts such as **8b** (*Fig. 7*) or **8a** (*Fig. 11*, below) than that of orange-brown bis-adduct **1**, with the broad band in the VIS region (λ_{max} 483 nm) becoming much stronger than the sharp absorption band at λ_{max} 421 nm. The spectra of tris-adducts **3** and **10** (*Fig. 10*) are similar in shape, but the major bands of **10** in the VIS are hypsochromically shifted; thus the relatively strong absorption of **3** at λ_{max} 498 nm appears at 462 nm in the spectrum of **10**.

iv) Multiple cylopropane fusion along an equatorial belt of the fullerene only weakly affects the HOMO-LUMO (optical) gap. A comparison between the red-brown bis- and tris(methano) derivatives **9** and **10** with the green-yellow tetrakis(methano)fullerene **11** (*Fig. 11*) revealed that, whereas band shapes and positions vary significantly, the end absorptions of all three compounds occur at nearly the same wavelength (λ_{max} *ca.* 650 nm). Thus, tetrakis-adduct **11** exhibits two weak bands with maxima at 573 (ε = 250) and 626 (ε = 200) nm. This is a clear indication that sequential cylopropane fusion along an equatorial belt perturbs only weakly the conjugated C_{60} π-chromophore, a conclusion previously also reached by *Asmus* and coworkers for isomeric bis-adducts [26a]. The influence of different addition patterns is once more reflected in the comparison between tetrakis-adducts **4** and **11**: whereas **11** with its conjugated π-chromophore of two biphenyl-type connected tetrabenzopyracyclene moieties (*Fig. 5*) shows its end absorption around 650 nm (*Fig. 11*), the end absorption of **4**, with its two localized benzenoid

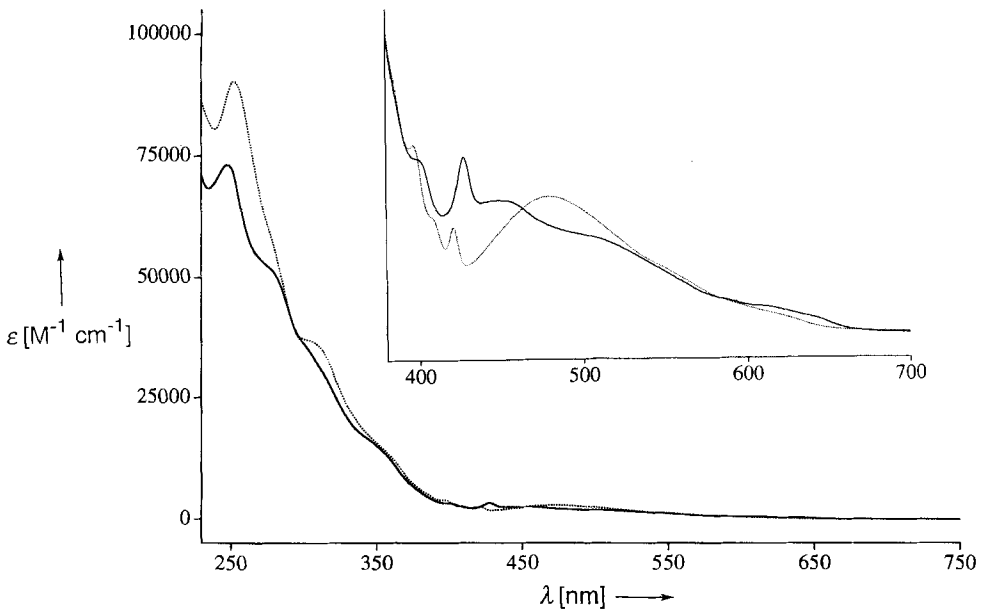

Fig. 9. *UV/VIS Spectra in CH_2Cl_2 of bis-adducts* **1** (——) *and* **9** (·····)

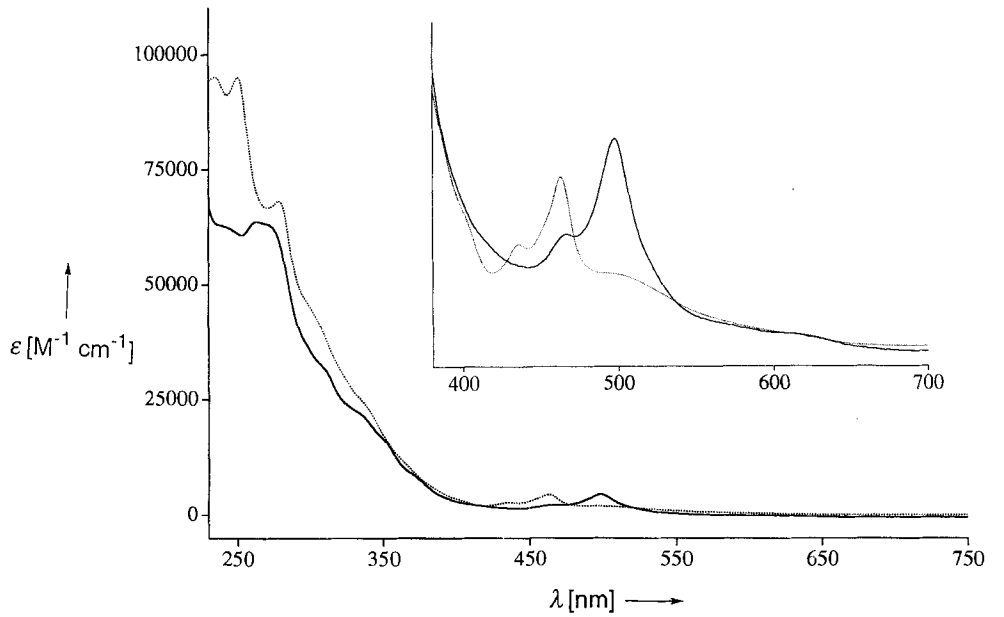

Fig. 10. *UV/VIS Spectra in CH_2Cl_2 of tris-adducts* **3** (——) *and* **10** (·····)

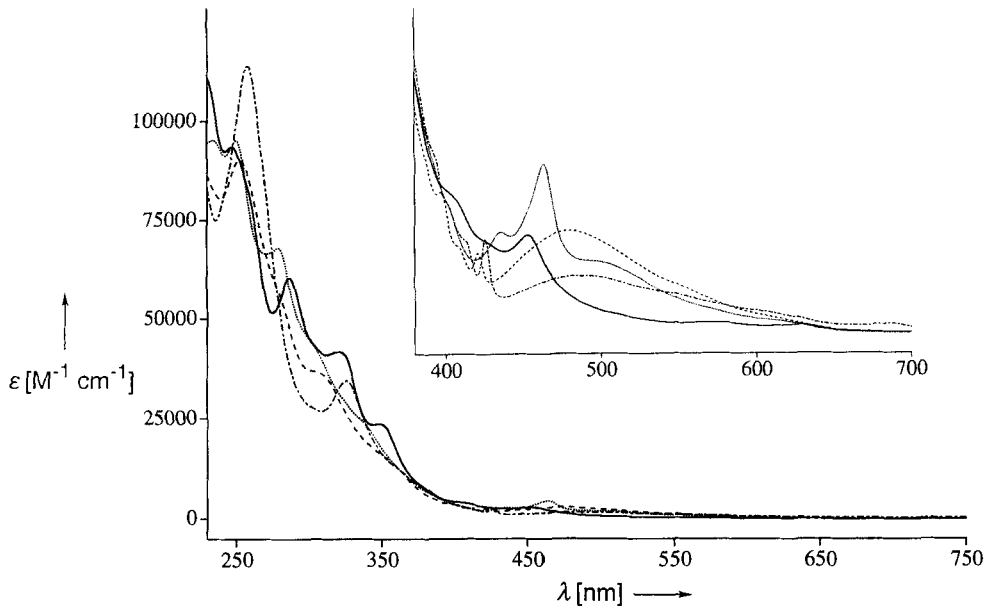

Fig. 11. *UV/VIS Spectra in CH_2Cl_2 of mono-adduct* **8a** (– · – · –), *bis-adduct* **9** (– – – –), *tris-adduct* **10** (· · · · · · · · ·), *and tetrakis-adduct* **11** (——)

rings (*Fig. 7*), occurs below 600 nm. Exclusive fusion along an equatorial belt as in **11** does not generate localized benzenoid rings which reduce the overall π-electron delocalization.

2.6.3. *Electrochemistry*. The electrochemical investigations on fullerene multiple adducts were carried out as described previously [3] by both cyclic (CV) and steady state voltammetry (SSV) in CH_2Cl_2 + 0.1M Bu_4NPF_6 on a glassy C electrode. The redox potentials determined by both methods were in mutually good agreement and are reported in *Table 1 vs.* the ferrocene/ferricinium couple (Fc/Fc^+). All redox processes discussed in the following are C-sphere-based. With a few exceptions [3] [4] [26], earlier electrochemical studies on covalent fullerene derivatives were focused on the more readily available mono- rather than multiple adducts of C_{60} [8] [10c] [18] [27].

The electrochemical study of mono- to hexakis-adducts **8b** and **2**–**7** had been previously published in detail [3]; therefore, only the most significant results from this series are included in the following discussion. Within the series of compounds included in *Table 1*, the following trends are apparent:

i) One-electron oxidation by CV is irreversible on the mono-adduct stage (**8b**, +1.23 V), then becomes increasingly facilitated up to the stage of tris-adduct **3** (+0.90 V), and then occurs at almost constant potential (+0.94 to +0.99 V) in all higher adducts. It seems attractive to propose that the benzenoid rings in the 'cubic' cyclophane substructure (*Fig. 7*) are the sites of oxidation leading to the observed, nearly constant oxidation potential.

Table 1. *Reduction and Oxidation Characteristics* (*vs.* Fc/Fc^+) *of Covalent Fullerene Adducts in Comparison to* C_{60} *on a Glassy Carbon Electrode in* $CH_2Cl_2 + 0.1$M Bu_4NPF_2. The degree of addition increases sequentially going down the *Table*.

	Cyclic voltammetry			Steady-state voltammetry (rotating disk electrode)				
	Reduction[a])			Oxidation[a])	Reduction[b])			Oxidation[b])
	E_1	E_2	E_3	E_1	E_1	E_2	E_3	E_1
C_{60}[c])	−0.98 (59)[d])	−1.37 (61)[d])	−1.83 (60)[d])		−0.98 (65)	−1.37 (65)	−1.83 (70)	
8b[c])	−1.06 (70)	−1.45 (70)	−1.94 (80)	+ 1.22[e])	−1.08 (63)	−1.47 (60)	−1.98 (51)	+ 1.23 (98)
2[c])	−1.18 (75)	−1.56 (75)	−2.20[e])	+ 1.04 (120)	−1.19 (80)	−1.56 (80)	−2.25 (90)	+ 1.04 (76)
24					−1.12 (68)	−1.50 (63)	−1.78 (60)[f])	
25					−1.12 (60)	−1.50 (68)	−2.02 (100)	
9	−1.11 (89)	−1.47 (94)	−2.15[e])	+ 1.2[e])	−1.13 (70)	−1.52 (72)	−2.15 (95)	+ 1.17 (94)
26					−1.11 (64)	−1.51 (62)	−2.02 (100)	
3[c])	−1.29 (78)	−1.67 (84)	−2.33[e])	+ 0.90 (92)	−1.30 (68)	−1.70 (67)		+ 0.90 (70)
23					−1.10 (62)	−1.49 (79)	< −2.2	
10	−1.12 (67)	−1.48 (77)	−2.21[e])	+ 1.09 (100)	−1.14 (60)	−1.50 (62)	−2.20 (77)	+ 1.09 (64)
4[c])	−1.53 (90)	−1.63 (70)		+ 0.98 (170)	−1.57 (119)			+ 0.98 (62)
11	−1.19 (75)	−1.54 (72)	−2.25[e])	+ 0.98 (75)	−1.19 (64)	−1.55 (59)	< −2.3	+ 0.98 (62)
5[c])	−1.57[e])	−2.27[e])		+ 0.99 (75)	−1.59 (98)	−2.30 (79)		+ 0.97 (60)
6[c])	−1.66[e])	−2.20[e])		+ 0.95 (100)	−1.66 (63)	−2.23 (84)		+ 0.94 (61)
7[c])	−1.87[e])			+ 0.99 (81)	−1.85 (131)			+ 0.98 (71)

[a]) Values quoted: $(E_pa + E_pc)/2$ in V and, in parenthesis, ΔE_pc in mV at 0.1 Vs^{-1}. For irreversible processes, E_pc in V is quoted. [b]) Values quoted: $E_{1/2}$ in V and, in parenthesis, the slope $\log(I/(I_d - I))$ in mV. [c]) Taken from [3]. [d]) Reduction on Pt electrode in $CH_2Cl_2 + 0.1$M Bu_4NPF_6. [e]) Irreversible process. [f]) Reduction of an electrogenerated species, a decomposition product of the dianion.

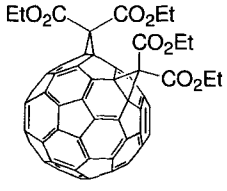

24 (*cis*-2)

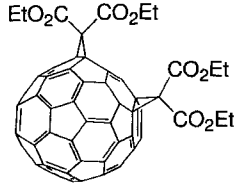

25 (*cis*-3)

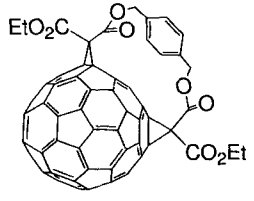

26 (*e*)

ii) In the series of mono- to hexakis-adducts **8b** and **2**–**7**, the number of reversible one-electron reductions measured in CH_2Cl_2 within the accessible potential range of +1.4 to −2.5 V *vs.* Fc/Fc^+ generally decreases with increasing number of addends and, concurrently, the first reduction occurs at increasingly negative potential. Whereas three reversible one-electron reductions were measured for mono-adduct **8b** (−1.08, −1.47, and −1.98 V), only one irreversible reduction was observed for hexakis-adduct **7** (−1.85 V). As the conjugated π-chromophore of the fullerene is increasingly reduced, the energy of the LUMO is raised (*Sect. 2.6.4*), making it more difficult to accept electrons in the electrochemical reduction.

iii) The nature of the fused addends has a significant influence on the first reduction potential. The *e*-bis-adducts **9** (−1.13 V) and **26** (−1.11 V), with two fused cyclopropane rings, are reduced more readily than **2** (−1.19 V) with one fused cyclopropane and one cyclohexene ring. Similarly on the tris-adduct stage, the reduction of **10** (−1.14 V) and **23** (−1.10 V) with three fused cyclopropane rings is much facilitated as compared to the reduction of **3** (−1.30 V) with one fused cyclopropane and two fused cyclohexene rings. Previous electrochemical studies of methanofullerenes essentially had shown that the reduction potentials were rather insensitive to the nature of the substituents at the methano moiety, since the sp^3-C-atom of this addend acts as an insulator [3] [10c] [27a–g]. This study provides first evidence that the nature of the fused addends has a strong influence on the reduction potentials.

iv) The regioisomeric position of the addends influences the reduction potential. Thus, there exists a large difference between the two regioisomeric pentakis-adducts **5** and **6**: compound **5** (−1.59 V) is reduced much more readily than **6** (−1.66 V) and almost at the same potential than tetrakis-adduct **4** (−1.57 V). Similarly, there exists a large difference between the tetrakis-adducts **4** and **11** with different addition patterns. Whereas compound **4** is reduced at −1.57 V, tetrakis(methano)fullerene **11** takes up an electron at the remarkably low potential of −1.19 V. A significant contribution to this difference in reduction potential certainly originates from the different conjugated π-chromophores in the two compounds, as discussed above (*Sect. 2.6.2*). However, it also needs to be considered that **11** possesses four fused cyclopropane rings whereas **4** is fused to two cyclopropane and two cyclohexene rings, and the comparisons among bis- and tris-adducts above clearly demonstrated that substitution of cyclohexene by cyclopropane rings facilitates electrochemical reduction.

On the bis-adduct stage, the regioisomerism does not yet seem to significantly influence fullerene redox properties: the first two reduction steps of **26** [9] and the three regioisomers **9**, **24**, and **25** [9] occur at nearly identical potential.

v) Multiple cyclopropane fusion along an equatorial belt has a remarkably small effect on the ability of the fullerene to accept electrons in electrochemical reductions: three one-electron reductions are observed in the series of mono- to tetrakis(methano)-fullerenes **8b** and **9**–**11**, and the first two reversible ones occur at similar potential (−1.08 to −1.19 V for the first and −1.47 to −1.55 V for the second electron transfer).

vi) We observe a significant correlation between the location of the end absorption (the optical HOMO-LUMO gap) in the UV/VIS spectra and the first reduction potential in electrochemistry. With increasing energy of the optical end absorption, the first reduction becomes increasingly difficult. Due to the strong tailing of the often very weak longest-wavelength absorptions, however, the optical gap cannot always be accurately determined.

2.6.4. *Computational Studies.* The geometries of all fullerene adducts were built using CHEMCAM [28]. To reduce the size of the computed molecules, cyclohexene rings were replaced by two H-atoms and malonate addends by a simple methano moiety. The structural and numbering correspondence between the experimentally investigated compounds **2**–**11** and the calculated structures **27**–**36** is shown in *Fig. 12.*

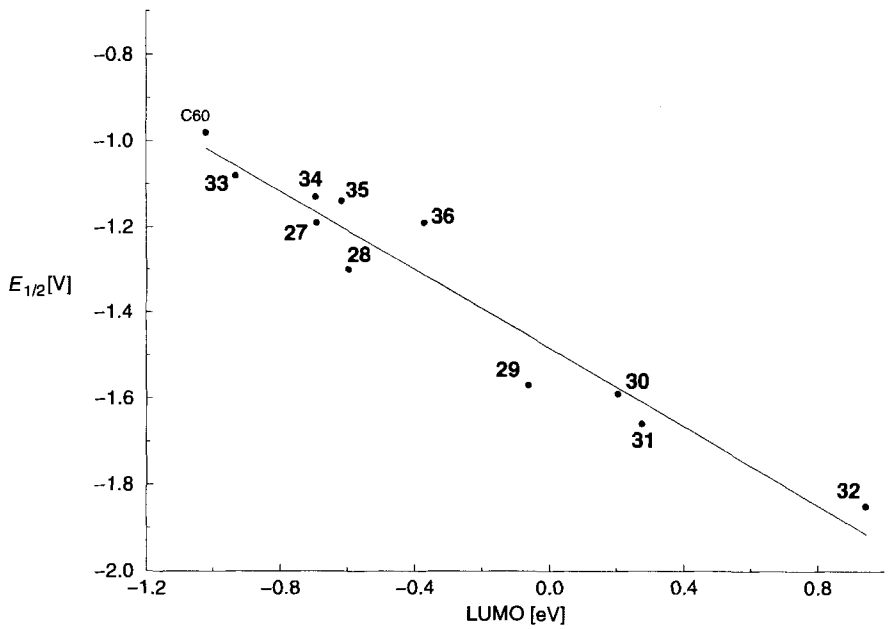

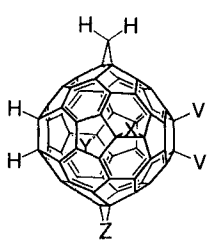

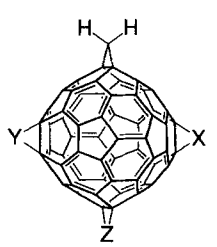

27 (**2**) VV = X = Y = Z = —
28 (**3**) V = H, X = Y = Z = —
29 (**4**) V = H, X = CH_2, Y = Z = —
30 (**5**) V = H, X = Z = CH_2, Y = —
31 (**6**) V = H, X = Y = CH_2, Z = —
32 (**7**) V = H, X = Y = Z = CH_2

33 (**8b**) X = Y = Z = —
34 (**9**) X = CH_2, Y = Z = —
35 (**10**) X = Y = CH_2, Z = —
36 (**11**) X = Y = Z = CH_2

Fig. 12. *First electrochemical reduction potentials* $E_{1/2}$ (SSV) *plotted as a function of LUMO energies from single point* ab-initio *RHF calculations with the 6-31G basis set.* The LUMO energies were computed for compounds **27**–**36** which are suitable models for the experimentally investigated fullerene adducts **2**–**11**. The compounds corresponding to the computed structures are indicated in parentheses. The correlation coefficient of the linear regression is $R = 0.97$.

The geometries were first optimized at the semi-empirical MNDO (*m*odified *n*eglect of *d*ifferential *o*verlap) [29] level using RHF-SCF (*r*estricted *Hartree-Fock s*elf-consistent *f*ield) calculations. Starting from the optimized structures, single-point *ab-initio* RHF calculations with the 6-31 G basis set were carried out using TURBOMOLE [30]. The energy values for the LUMO orbitals obtained by the semi-empirical and the *ab-initio* methods were plotted *vs.* the experimental first reduction potential. In both graphs, a very good correlation between the reduction potentials $E_{1/2}$ measured by SSV for compounds **2**–**11** and the LUMO energies calculated for **27**–**36** was obtained as is shown for the *ab-initio* calculated values in *Fig. 12*.

In preliminary studies, MNDO electron affinities were computed from the energy difference between optimized structures of the anions and neutral molecules. The calculations for the open-shell anions made use of the half-electron ROHF (*r*estricted *o*pen-shell *Hartree-Fock*) treatment and employed analytical gradients [31]. The MNDO electron affinity of C_{60} (-62.4 kcal mol^{-1}) is very close to the experimental value of -61.1 ± 1.2 kcal mol^{-1} [32]. In the series from C_{60} to pentakis-adducts (**33** and **27**–**31** corresponding to **8b** and **2**–**6**), an excellent correlation between the calculated electron affinities and the measured first reduction potential was obtained (*Fig. 13*).

2.6.5. *IR and NMR Spectroscopy.* In the IR spectra (KBr) of *all* multiple adducts discussed in this paper, the most prominent of the four absorptions seen in the spectrum of C_{60} [33] at 528 cm^{-1} is maintained and appears as a strong band in the narrow range between 524 and 531 cm^{-1}. This vibration in C_{60} was assigned to a pure radial breathing mode [34], and a similar origin can be assumed for the adducts. Apparently, this breath-

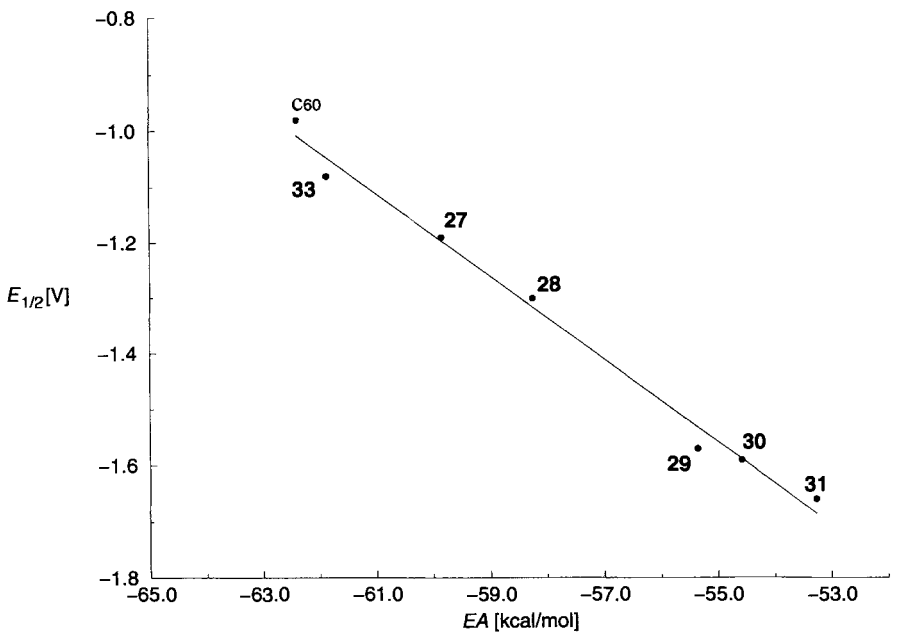

Fig. 13. *First electrochemical reduction potentials* $E_{1/2}$ (SSV) *plotted as a function of the electron affinities calculated at the MNDO level* (see text). For the numbering of compounds, see *Fig. 12*. The correlation coefficient of the linear regression is $R = 0.99$.

ing mode of the C-sphere is quite insensitive to degree, pattern, and nature of functionalization.

^{1}H-NMR Resonances of protons near the fullerene surface are particularly affected by the paramagnetic ring currents associated with the pentagons [35]. These ring currents shift the resonances of protons located atop or in close proximity to pentagons strongly downfield [22b] [36]. With each addition to central 6-6 bonds of pyracylene subunits in C_{60}, the full π-electron delocalization within two pentagons becomes interrupted and, therefore, we expected higher functionalization to reduce the deshielding of protons located atop the C-sphere. Furthermore, as more addends are attached, the shielding influence of developing isolated benzenoid six-membered rings becomes increasingly important.

Table 2. *Selected ^{1}H-NMR Data* (ppm) *for a Series of Mono- through Hexakis-adducts in $CDCl_3$.* The cyclohexene CH_2 group near the anchor is labeled *p* (proximal), the one farther away *d* (distal).

	37[a])	**2**[b])	**3**[c])	**4**	**5**	**6**	**7**
Benzyl CH_2O	–	5.25	5.18	5.19	5.30	5.12	5.22
=C–H	6.59	6.55	6.52	6.41	6.27	6.30	6.16
CH_2 (*p*)	3.98	3.48	3.42	3.28, 3.18	3.22, 3.12	3.07	2.95
CH_2 (*d*)	3.99	3.72	3.80	3.60, 3.56	3.45, 3.34	3.44	3.21

[a]) Taken from [12a]. [b]) Measured in $CDCl_3/CS_2$ 1:1. [c]) Measured in $C_2D_2Cl_4$.

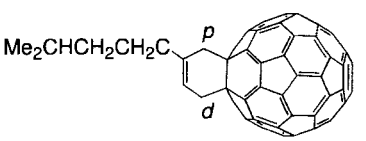

37

Significant changes in chemical shift, which can be rationalized by both effects, were found in the comparison of the ^{1}H-NMR spectra of *Diels-Alder* adducts **37** [12a] and **2**–**7** (*Table 2*). Whereas the benzylic CH_2O protons are not much affected by the degree of addition, the resonances of the proximal (*p*) and distal (*d*) CH_2 groups of the cyclohexene moieties and the alkenyl protons shift upfield with increasing functionalization. At more than 1 ppm, the change in chemical shift of the proximal CH_2 protons, when passing from mono- to hexakis-adduct, is the most substantial one (*Table 2*).

A large influence of degree and pattern of addition on the ^{3}He-NMR chemical shifts of endohedral ^{3}He complexes of **2**–**7** were also encountered. As a general trend, the ^{3}He resonances move upfield with increasing number of addends; these findings are reported elsewhere [37].

An interesting observation was made in the comparison of ^{13}C-NMR spectra. Whereas the fullerene sp^2-C-atom resonances in all adducts of this study start appearing around 138–139 ppm, their range extends much more downfield when the C-sphere is fused to cyclohexene rings, derived from *Diels-Alder* addition, than if it is fused to cyclopropane rings only. Whereas the range of the sp^2-C-atom resonances in the spectra of exclusively cyclopropane-fused derivatives such as **8**–**11** and, similarly, of the multiple diethyl malonate adducts studied by *Hirsch et al.* [5] [7] [10a] [24] extends to a maximum of 148 ppm, the spectra of *Diels-Alder* adducts such as **37** or **2**–**7** displayed these

resonances as far downfield as 158–160 ppm. Similarly, the pseudo-octahedral hexakis(methano) adduct **38** of *Hirsch et al.* [7] depicted two fullerene sp^2-C-atom resonances at 141.13 and 145.78 ppm, whereas the corresponding hexakis(*Diels-Alder*) adduct **39**, reported by *Kräutler* and *Maynollo* [12b] showed the same two resonances at 142.0 and 152.0 ppm. It is noticeable that the ^{3}He-NMR resonances in endohedral ^{3}He complexes of cyclopropane- and cyclohexane-fused fullerene derivatives also appear at significantly different chemical shifts [38].

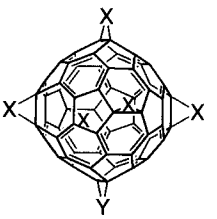

38 X = Y = $(EtO_2C)_2C$

39 X = Y = 

40 X = $(EtO_2C)_2C$, Y = ——

2.6.6. *Chemical Reactivity.* Significant changes in chemical reactivity as a function of degree and pattern of addition and the nature of the fused addends were observed. With a raise in LUMO energy, the electrophilicity of the C-sphere decreases and, as a consequence, its reactivity in reactions with nucleophiles and nucleophilic carbenes, or as dienophile in cycloadditions is reduced. Thus, we found in the preceding study [1] that, in contrast to C_{60}, tris-adduct **3** no longer underwent a *Diels-Alder* reaction with anthracene and also did not react with dimethoxycarbene. Polar additions such as *Bingel*-type reactions [6a] [39] to higher C_{60} adducts required the use of polar solvents such as Me_2SO to decrease their activation barriers, whereas additions to C_{60} and lower adducts were best performed in PhMe or CH_2Cl_2. In contrast to mono-adducts, hexakis-adducts no longer reacted with the nucleophilic F^- anion. The ability of covalent fullerene derivatives to act as photosensitizers for $^1O_2$ formation decreases with increasing number of addends, and the efficient sensitization of the $^1O_2$ ene reaction of **7** (*Sect. 2.1*) required addition of C_{60} as photosensitizer to the reaction.

Additional examples illustrate the nice correlations between electrochemical reduction potentials and LUMO energies on the one and electrophilic reactivity on the other side. Despite a large excess of nucleophilic reagent (5 equiv.), the *Bingel* reaction of diethyl 2-bromomalonate and 1,8-diazabicyclo[5.4.0]undec-7-ene (DBU) in PhCl with tris-adduct **3** to give tetrakis-adduct **4** was very clean, not producing any higher adducts [1]. The reduction potential of **4** ($E_1 = -1.57$ V) is 0.24 V more negative than that of **3** ($E_1 = -1.30$ V) and, accordingly, **3** shows greatly enhanced electrophilic reactivity over **4**. In contrast, formation of pentakis-adducts such as **5** (28%; $E_1 = -1.59$ V) and **6** (11%; $E_1 = -1.66$ V) by *Bingel* addition to the corresponding tetrakis-adduct (similar to **4**; $E_1 = -1.57$ V) always yielded substantial amounts of hexakis-adduct, since the reduction potentials and, hence, the electrophilicity of tetrakis- and pentakis-adducts, in particular **4** and **5**, are quite similar.

Tetrakis(methano)fullerene **11** ($E_1 = -1.19$ V) is more reactive than the tetrakis-adduct **4** ($E_1 = -1.57$ V). When in a competition experiment, a 1:1 mixture of the two compounds was reacted with diethyl 2-bromomalonate (1 equiv.) and DBU (1 equiv.) in PhCl, the ratio of recovered material **4**/**11** was 2.7:1 and pentakis-adduct **40** [7], formed from **11**, had almost completely reacted to give hexakis-adduct **38** [7]. That differences in the nature of the fused addends alone have a significant effect on reactivity was demonstrated in a comparison between the pentakis-adducts **40** and **6**. In the reaction with a large excess of diazomethane in CH_2Cl_2, conversion of pentakis(methano)fullerene **40** was completed within 15 min, whereas, under identical conditions, **6** took 90 min to react to completion [40].

2.6.7. *The Different Effects on Physical Properties and Chemical Reactivity Caused by Cyclopropane and Cyclohexene Fusion to C_{60}.* In this work, a major difference between the effects of cyclopropane and cyclohexene fusion on fullerene properties was revealed. As compared to cyclohexene fusion, anellation by a cyclopropane ring leads to a lower-energy optical gap in the UV/VIS spectrum, facilitated electrochemical reduction, lower LUMO energy, and enhanced electrophilic reactivity. In addition, the resonances of fullerene sp^2-C-atoms, presumably those connected to the fusion-site C-atoms, appear in a different range in the ^{13}C-NMR spectra. We attribute these differences to the particular character of the methano moieties. The analysis of the X-ray crystal structure of hexakis-adduct **7**, which contains both cyclopropane and cyclohexene rings, showed [17] that the angular strain, which reflects the degree of pyramidalization, is significantly larger for the fusion-site C-atoms in the cyclohexene ring. The deformations produced in the five- and six-membered rings within the bridged pyracylene subunits by the *Diels-Alder* addition are also more pronounced than those resulting from the methano bridging. Such steric effects could well explain the observed differences in the location of the sp^2-C-atoms resonances in the ^{13}C-NMR spectrum and, to some extent, the differences in electronic properties. However, we feel that the latter might rather result from the particular nature of the fused cyclopropane rings which resemble those in small [*n.n.*1]propellanes [41]. Although of a relatively short distance, the fusion bond in the cyclopropane rings is subject to considerable variation as observed in the X-ray crystal structure of **11** (*Sect. 2.2*) and could possibly be considered a weaker than normal C–C bond, as had been discussed for [1.1.1]propellane [42]. Actually, the effective bridgehead or fusion C–C single-bond strength in both [1.1.1]propellane as well as in 6-6-closed methanofullerenes seems not to be established. A weaker than normal fusion bond would explain the reduced perturbation of the fullerene π-chromophore caused by the methano moiety at 6-6 bonds and, correspondingly, the remarkable conservation of characteristic fullerene type properties such as facile reducibility, low-lying LUMO, and high electrophilic reactivity in methano adducts such as **8**–**11**. The particular properties of 6-6-closed methanofullerenes would also be consistent with the well-established notion, that cyclopropanes 'have properties that are similar (in certain ways) to double bonds' [38].

3. Conclusion. – With the removal of the tether, an important extension of the tether-directed remote functionalization of C_{60} was accomplished providing access to fullerene multiple adducts such as **10** and **11** with addition patterns that cannot be accessed without tether or template assistance. Thus, a series of C_{60} mono- to tetra-

kis(methano)fullerenes **8**–**11**, in which all methano moieties are attached along an equatorial belt, could be completed. Derivatives of **11** with long-chain alkyl esters (**16** and **17**) are noncrystalline under ambient conditions, and the insertion of mesogenic moieties into the ester residues promises to yield novel fullerene-containing liquid-crystalline materials [21]. The X-ray crystal structure of a $CHCl_3$ solvate of **11** was solved and showed a slight reduction of the conjugated fullerene π-chromophore to two tetrabenzopyracylene substructures connected by four biphenyl-type bonds. In the eight six-membered rings fused to the two pyracyclene moieties, 6-6 and 6-5 bond-length alteration (0.05 Å) was found to be reduced by *ca.* 0.01 Å with respect to the free C_{60} skeleton (0.06 Å). The analysis of the crystal packing revealed interesting short contacts between Cl-atoms of the solvent and sp^2- and sp^3-C atoms of the C-sphere, besides short contacts between the Cl-atoms and O-atoms of the malonate addends.

The physical properties and chemical reactivity in the series of methanofullerenes **8**–**11** and the previously prepared series of bis- to hexakis-adducts **1**–**7** [1–3] were comprehensively analyzed as a function of degree and pattern of addition as well as the nature of the fused addends. Strong correlations and trends were revealed. With increasing reduction in the conjugated fullerene π-chromophore, *i*) the optical (HOMO-LUMO) gap in the UV/VIS spectrum shifts to higher energy, *ii*) the number of reversible one-electron reductions decreases and the first reduction potential becomes increasingly negative, *iii*) the computed LUMO energy increases and the electron affinity decreases, *iv*) the reactivity of the fullerene towards nucleophiles and carbenes or as dienophile in cycloadditions decreases, and *v*) the capacity for photosensitization of $^1O_2$ formation decreases. The hypsochromic shift of the optical gap is particularly pronounced if localized benzenoid rings are generated in the fullerene chromophore as a result of the functionalization. Furthermore, the nature of the addition pattern and, quite remarkably, the nature of the fused addends affects the above mentioned properties. We found a strong difference between cyclopropane- and cyclohexene-fused fullerenes: in general, all-cyclopropene-fused fullerenes exhibited a lower-energy optical gap, more reversible one-electron reductions at less negative potential, lower LUMO energies and higher electrophilic reactivity, as compared to compounds fused to cyclohexene rings. Apparently, a methano moiety at a 6-6-closed bond represents a smaller perturbation of a fullerene chromophore than a but-2-ene-1,4-diyl moiety at such a bond. The smallest perturbation of the fullerene π-chromophore by multiple additions seems to occur when all methano addends are sequentially introduced along an equatorial belt as in the series **8**–**11**. Thus, tetrakis(methano)fullerene **11** closely resembles the corresponding bis-adduct **9** in its optical gap, reduction potentials, and LUMO energy. Overall, a remarkably good correlation between optical gap, LUMO energy, reduction potential, and chemical reactivity holds within the entire series of compounds considered, independent of their differences in degree and pattern of addition and nature of addends.

The study revealed a strong preservation of the radial breathing mode observed in the IR spectrum of C_{60} at 528 cm^{-1}; this strong vibration appears in the spectra of multiple adducts between 524 and 531 cm^{-1}. Also, upon increasing degree of addition, protons located atop the fullerene sphere shift increasingly upfield in the ^{1}H-NMR spectrum, presumably due to the reduction in the number of pentagons with paramagnetic ring currents and the increase in the number of localized benzenoid rings. Finally, cyclopropane- and cyclohexene-fused adducts also differ in the location of the fullerene

sp^2-C-atom resonances in the ^{13}C-NMR spectra: whereas in the former, these resonances expand downfield to *ca.* 148 ppm, they appear in the *Diels-Alder* adducts as far downfield as 160 ppm.

The development of the (reversible) tether-directed remote functionalization method yielded with high regioselectivity a unique series (**1**–**11**) of fullerene multiple adducts. Clearly, the C-sphere is increasingly becoming a useful template for the covalent attachment of functional groups in three dimensions, and multiply functionalized compounds for materials and biological applications are now in reach. In addition, the good access to many different degrees and patterns of functionalization by this elegant synthetic strategy has opened the way to the first comprehensive comparative study of physical properties and chemical reactivity in covalent fullerene chemistry.

Experimental Part

General. See [1]. Compounds **4**, **5** and **7** were prepared according to literature procedures [1]. Photosensitization experiments were performed with a medium-pressure Hg lamp in a *Pyrex* photochemical reactor. The electrochemical investigations were carried out as previously described [3]. HPLC Columns: *Spherisorb S W* SiO_2 (5 μm), 250 mm × 4 mm i.d.; *Spherisorb S W* SiO_2 (5 μm), 250 mm × 20 mm i.d. Anal. HPLC: *Merck-Hitachi* HPLC pump *L6200A; Merck-Hitachi* UV detector *L4250; Merck-Hitachi* integrator *D2500;* flow rate 2 ml min^{-1}. Prep. HPLC: *Merck-Hitachi* HPLC pump *L6250; Merck-Hitachi* UV detector *L4000; Merck-Hitachi* integrator *D2500;* flow rate 10 ml min^{-1}. All HPLC chromatograms were taken at r.t. with the detector wavelength fixed at λ 254 nm. LDI-TOF-MS (*m/z*): spectra with reflectron detection were measured in the positive- or negative-ion mode, acceleration voltage 15 kV, on a *Bruker REFLEX* spectrometer.

*3',3'-Bis{{4-{2-[3,4-bis(methoxycarbonyl)phenyl]ethyl}phenyl}methyl} 3'',3''',3'''',3''''',3''''',3''''''-Hexaethyl 3'*H,*3''*H,*3'''*H,*3''''*H-*Tetracyclopropa[1,9:16,17:44,45:52,60][5,6]fullerene-*C_{60}-I_h-*3',3',3'',3'',3''',3''',3'''',3''''',3''''''-octacarboxylate* (**15**). A soln. of **7** (200 mg, 0.122 mmol) and C_{60} (102 mg, 0.142 mmol) in PhCl (160 ml) was irradiated in a photochemical reactor at r.t. for 2 h, while a stream of O_2 was bubbled through. The mixture **12** (R_f 0.43; TLC, SiO_2, CH_2Cl_2/AcOEt 9:1) was then transferred into a flask and deoxygenated by inserting a stream of Ar, and PPh_3 (320 mg, 1.221 mmol) in PhCl (5 ml) was added. After stirring at r.t. for 1 h under Ar, plug filtration (SiO_2) with PhMe to remove PhCl and C_{60}, then with CH_2Cl_2/AcOEt 19:1 and then 9:1, yielded **13**, which was precipitated out of CH_2Cl_2 by addition of hexane: 183 mg (90%). MALDI-TOF-MS (CCA): 1669 (M^+; calc. for $^{13}C^{12}C_{109}H_{60}O_{12}$: 1669). To isolate and fully characterize one of the formed constitutional isomers, the mixture was separated by CC (SiO_2, CH_2Cl_2/AcOEt 19:1), instead of performing the above described plug filtration, and the first of three main yellow fractions was collected. CC (SiO_2-*H*, CH_2Cl_2/AcOEt 23:2) of this fraction yielded the constitutional isomer of **13** shown in *Scheme 2* as a mixture of *meso-* and *rac*-diastereoisomers. Yellow solid. ^1H-NMR (500 MHz, $CDCl_3$): 1.25 (*tm*, *J* = 7.1), 1.280 (*tm*, *J* = 7.1), 1.289 (*tm*, *J* = 7.1), 1.30 (*tm*, *J* = 7.0), 1.35 (*tm*, *J* = 7.1), 1.41 (*tm*, *J* = 7.1), 32H; 1.95–2.10 (*m*, 4H); 2.14–2.24 (*m*, 4H); 2.43–2.57 (*m*, 4H); 2.58–2.70 (*m*, 4H); 2.86–2.95 (*m*, 4H); 3.12–3.22 (*m*, 4H); 4.23 (*qm*, *J* = 7.1), 4.27 (*qm*, *J* = 7.1), 4.31 (*qm*, *J* = 7.1), 4.37 (*qm*, *J* = 7.0), 4.39 (*qm*, *J* = 7.1), 4.41 (*qm*, *J* = 7.1), 24H; 4.89 (*d*, *J* = 11), 4.93 (*d*, *J* = 11), 5.46 (*d*, *J* = 11), 5.51 (*d*, *J* = 11), 8H; 6.17 (*d*, *J* = 9.8, 4H); 6.26 (*d*, *J* = 9.8, 4H); 7.00–7.08 (*m*, 8H); 7.17–7.22 (*m*, 4H); 7.30–7.38 (*m*, 4H). MALDI-TOF-MS (CCA): 1669 (M^+; calc. for $^{13}C^{12}C_{109}H_{60}O_{18}$: 1669).

TsOH (54 mg, 0.285 mmol) and DMAD (135 mg, 0.950 mmol) were added to a soln. of the isomer mixture **13** (159 mg, 0.095 mmol) in deoxygenated PhMe (200 ml), and the mixture was refluxed for 4.5 h in the dark. CC (SiO_2, CH_2Cl_2 followed by CH_2Cl_2/AcOEt 49:1 then 24:1) yielded **15** as a yellow-green product, that was precipitated from CH_2Cl_2 by addition of hexane: 86 mg (47%). Bronze solid. M.p. > 205° (dec.). UV/VIS (CH_2Cl_2): 627 (170), 574 (310), 453 (2700), 430 (sh, 2650), 405 (sh, 4050), 346 (sh, 22400), 318 (39700), 286 (59100), 245 (sh, 104100). IR (KBr): 2978*m*, 2933*m*, 2844*w*, 1739*s*, 1722*s*, 1605*w*, 1517*w*, 1433*m*, 1389*w*, 1362*w*, 1289*s*, 1250*s*, 1211*s*, 1128*m*, 1068*s*, 1017*m*, 856*w*, 811*w*, 761*w*, 739*w*, 711*w*, 673*w*, 583*w*, 539*w*, 528*m*. ^1H-NMR (500 MHz, $CDCl_3$): 1.43 (*t*, *J* = 7.1, 6H); 1.44 (*t*, *J* = 7.1, 6H); 1.45 (*t*, *J* = 7.1, 6H); 2.90 (*m*, 8H); 3.88 (*s*, 6H); 3.90 (*s*, 6H); 4.49 (*q*, *J* = 7.1, 4H); 4.51 (*q*, *J* = 7.1, 4H); 4.52 (*q*, *J* = 7.1, 4H); 5.37 (*s*, 4H); 7.11 (*dm*, *J* = 8.1, 4H); 7.26 (*dd*, *J* = 7.9, 1.8, 2H); 7.30 (*dm*, *J* = 8.1, 4H); 7.49 (*d*, *J* = 1.8, 2H); 7.65 (*d*, *J* = 7.9, 2H). ^{13}C-NMR (125.8 MHz, $CDCl_3$): 14.06; 14.13; 14.15; 36.95; 37.36; 43.91; 44.29; 46.84; 52.47; 52.60; 63.12; 63.14; 63.18; 68.52; 69.86; 69.97; 71.16; 128.55; 128.60; 129.12; 129.20; 129.26; 130.87; 132.62; 132.68; 140.77; 140.83; 141.43; 141.89;

142.20; 142.41; 142.42; 142.52; 142.65; 144.22; 144.24; 144.32; 145.37; 145.40; 145.41; 163.68; 163.82; 164.07; 164.12; 167.65; 168.39. MALDI-TOF-MS (CCA): 1916 (M^-; calc. for $^{13}C^{12}C_{121}H_{68}O_{24}$: 1917). HR-FAB-MS: 1916.4090 (M^+, $^{12}C_{122}H_{68}O_{24}{}^+$; calc. 1916.4100).

Octaethyl 3'H,3''H,3'''H,3''''H-Tetracyclopropa[1,9:16,17:44,45:52,60][5,6]fullerene-C_{60}-I_h-3',3',3'',3'',3''',3''',3'''',3''''-octacarboxylate (**11**). To a soln. of **15** (30 mg, 0.0156 mmol) in anh. EtOH/THF 1:1 (30 ml) was added K_2CO_3 (155 mg, 1.123 mmol), and the mixture was stirred at r.t. under Ar for 3.5 h. After filtration and evaporation, CC (SiO_2, CH_2Cl_2/AcOEt 19:1) afforded **11** which was precipitated from CH_2Cl_2 by addition of hexane: 17 mg (80%). Bronze solid. M.p. > 270°. UV/VIS (CH_2Cl_2): 626 (200), 573 (250), 453 (2850), 428 (sh, 2650), 409 (sh, 3750), 348 (sh, 23700), 320 (41700), 287 (60400), 245 (93600). IR (KBr): 2977*m*, 2922*m*, 2856*w*, 1741*s*, 1630*w*, 1466*w*, 1389*w*, 1366*m*, 1251*s*, 1213*s*, 1174*m*, 1097*m*, 1075*s*, 1020*m*, 910*w*, 860*w*, 740*w*, 717*w*, 679*w*, 583*w*, 540*w*, 527*m*. ^{1}H-NMR (500 MHz, $CDCl_3$): 1.44 (*t*, *J* = 7.1, 12H); 1.46 (*t*, *J* = 7.1, 12H); 4.50 (*q*, *J* = 7.1, 8H); 4.52 (*q*, *J* = 7.1, 8H). ^{13}C-NMR (125.8 MHz, $CDCl_3$): 14.14; 14.16; 44.28; 46.83; 63.12; 63.17; 69.98; 71.17; 140.87; 142.20; 142.45; 142.64; 144.24; 144.35; 145.44; 163.86; 164.15. LDI-TOF-MS: 1353 (M^-; calc. for $^{12}C_{88}H_{40}O_{16}$: 1352). HR-FAB-MS: 1352.2321 (M^+, $^{12}C_{88}H_{40}O_{16}{}^+$; calc. 1352.2316).

Octadecyl 3'H,3''H,3'''H,3''''H-Tetracyclopropa[1,9:16,17:44,45:52,60][5,6]fullerene-C_{60}-I_h-3',3',3'',3'',3''',3''',3'''',3''''-octacarboxylate (**16**). A mixture of **15** (34 mg, 0.017 mmol), dodecan-1-ol (17 ml, 75.805 mmol), and Cs_2CO_3 (462 mg, 1.418 mmol) in THF (17 ml) was stirred at r.t. under Ar for 1 d. After filtration and evaporation, CC (2 ×; SiO_2, CH_2Cl_2/hexane 1:1) yielded as the first yellow fraction a mixture of **16** and mono-decarboxylated material. The two products were separated by prep. HPLC (SiO_2, CH_2Cl_2/hexane 1:1), and the second fraction afforded pure **16** (6 mg, 14%). Viscous yellow-brown material. TLC (SiO_2, CH_2Cl_2/hexane 1:1): R_f 0.66. UV/VIS (CH_2Cl_2): 626 (500), 573 (520), 453 (1700), 429 (1650), 409 (sh, 2200), 348 (sh, 11300), 319 (19800), 286 (28700), 245 (44400). IR ($CHCl_3$): 2956*m*, 2911*s*, 2844*m*, 1733*m*, 1600*w*, 1461*w*, 1261*s*, 1100*m*, 1017*m*, 872*w*, 694*w*, 637*w*. ^{1}H-NMR (300 MHz, $CDCl_3$): 0.80–0.94 (*m*, 24H); 1.15–1.48 (*m*, 144H); 1.72–1.88 (*m*, 16H); 4.35–4.48 (*m*, 16H). ^{13}C-NMR (125.8 MHz, $CDCl_3$): 14.05; 22.64; 25.92; 28.55; 29.23; 29.25; 29.32; 29.56; 29.61; 29.65; 31.88; 44.51; 46.99; 67.20; 67.28; 70.06; 71.24; 140.85; 142.26; 142.48; 142.62; 144.22; 144.34; 145.42; 163.94; 164.21. FAB-MS: 2475 (100, MH$^+$; calc. for $^{13}C^{12}C_{167}H_{201}O_{16}$: 2475), 2289 (33, $[M - (O(CH_2)_{11}CH_3)]^+$).

Octaoctyl 3'H,3''H,3'''H,3''''H-Tetracyclopropa[1,9:16,17:44,45:52,60][5,6]fullerene-C_{60}-I_h-3',3',3'',3'',3''',3''',3'''',3''''-octacarboxylate (**17**). A mixture of **15** (30 mg, 0.015 mmol), octan-1-ol (15 ml, 94.909 mmol), and Cs_2CO_3 (407 mg, 1.251 mmol) in THF (15 ml) was stirred at r.t. under Ar for 6 h. After filtration and bulb-to-bulb distillation (55°/0.5 Torr) to remove unreacted octan-1-ol, CC (SiO_2, CH_2Cl_2/hexane 1:1) afforded as the first yellow band a mixture of **17** and mono-decarboxylated products, which was purified by prep. HPLC (SiO_2, CH_2Cl_2/hexane 3:2) to give as second fraction pure **17** (5 mg, 16%). Viscous yellow-brown material. TLC (SiO_2, CH_2Cl_2/hexane 1:1): R_f 0.56. UV/VIS (CH_2Cl_2): 625 (280), 573 (340), 453 (1800), 428 (sh, 1750), 409 (sh, 2400), 348 (sh, 13700), 320 (23800), 287 (34500), 247 (53400). IR ($CHCl_3$): 2945*m*, 2922*s*, 2844*m*, 1733*s*, 1600*m*, 1461*w*, 1256*s*, 1100*m*, 1006*m*, 873*w*, 696*w*, 639*w*. ^{1}H-NMR (300 MHz, $CDCl_3$): 0.78–0.98 (*m*, 24H); 1.15–1.50 (*m*, 80H); 1.72–1.88 (*m*, 16H); 4.32–4.48 (*m*, 16H). ^{13}C-NMR (125.8 MHz, $CDCl_3$): 14.03; 22.60; 25.90; 25.91; 28.53; 28.55; 29.18; 29.65; 31.76; 44.47; 46.95; 67.21; 67.27; 70.06; 71.24; 140.85; 142.27; 142.48; 142.63; 144.22; 144.34; 145.42; 163.95; 164.21. FAB-MS: 2026 (100, M^+; calc. for $^{13}C^{12}C_{135}H_{136}O_{16}$: 2026), 1896 (21, $[M - O(CH_2)_7CH_3]^+$), 720 (7, C_{60}^+).

3',3'-Bis{{4-{2-[3,4-bis(methoxycarbonyl)phenyl]ethyl}phenyl}methyl} 3'',3''-Diethyl 3'H,3''H-Dicyclopropa[1,9:16,17][5,6]fullerene-C_{60}-I_h-3',3',3'',3'',3''-tetracarboxylate (**20**). A soln. of **4** (70 mg, 0.053 mmol) and C_{60} (44 mg, 0.061 mmol) in PhCl (65 ml) was irradiated in a photoreactor at r.t. for 2 h, while O_2 was bubbled through. The mixture (TLC (SiO_2, CH_2Cl_2/AcOEt 19:1): R_f 0.26, 0.34) was transferred into a flask and deoxygenated with Ar, and PPh_3 (139 mg, 0.530 mmol) in PhCl (4 ml) was added. After stirring at r.t. for 1 h under Ar, plug filtration (SiO_2) with CH_2Cl_2 to remove PhCl and C_{60}, then with CH_2Cl_2/AcOEt 19:1 and then 9:1, yielded a red soln. that was concentrated and dried to give **19** (52 mg, 72%). MALDI-TOF-MS (CCA): 1353 (100, M^+; calc. for $^{13}C^{12}C_{95}H_{40}O_{10}$: 1353), 1336 (28, $[M - H_2O]^+$).

The isomer mixture **19** (51 mg, 0.037 mmol), TsOH (21 mg, 0.113 mmol), and DMAD (53 mg, 0.377 mmol) were heated to reflux in deoxygenated PhMe (80 ml) for 4.5 h in the dark. After 14 h at r.t., CC (SiO_2, CH_2Cl_2 then CH_2Cl_2/AcOEt 24:1) yielded a red-brown product that was precipitated from CH_2Cl_2 by addition of hexane: **20** (12 mg, 20%). Brown solid. M.p. > 200°. UV/VIS (CH_2Cl_2): 483 (2050), 421 (1150), 409 (sh, 1250), 397 (2450), 358 (sh, 11200), 306 (sh, 33500), 279 (sh, 55000), 250 (93500). IR (KBr): 2947*m*, 2845*w*, 1722*s*, 1606*m*, 1572*w*, 1511*w*, 1428*s*, 1367*m*, 1283*s*, 1239*s*, 1194*s*, 1117*s*, 1095*s*, 1067*s*, 1017*m*, 806*m*, 761*w*, 739*w*, 706*m*, 668*w*, 583*w*, 556*m*, 527*s*. ^{1}H-NMR (500 MHz, $CDCl_3$): 1.36 (*t*, *J* = 7.1, 3H); 1.41 (*t*, *J* = 7.1, 3H); 2.89 (*m*, 8H); 3.86 (*s*, 6H); 3.88 (*s*, 6H); 4.41 (*q*, *J* = 7.1, 2H); 4.47 (*q*, *J* = 7.1, 2H); 5.30 (*d*, *J* = 11.9, 2H); 5.36 (*d*, *J* = 11.9, 2H); 7.10 (*dm*, *J* = 8.0, 4H); 7.24 (*dd*, *J* = 7.9, 1.7, 2H); 7.27 (*dm*, *J* = 8.0, 4H); 7.47 (*d*, *J* = 1.7, 2H); 7.63 (*d*, *J* = 7.9, 2H).

^{13}C-NMR (125.8 MHz, $CDCl_3$): 14.11; 14.17; 36.97; 37.37; 49.09; 52.53; 52.66; 63.20; 63.22; 68.61; 70.20; 71.42; 71.63; 128.64; 128.65; 129.16; 129.23; 129.30; 130.90; 132.54; 132.71; 138.59; 138.82; 141.48; 141.56; 141.65; 141.83; 142.36; 142.85; 142.98; 143.07; 143.33; 143.61; 143.76; 143.99; 144.08; 144.35; 144.44; 144.58; 144.63; 144.68; 145.00; 145.14; 145.33; 145.38; 145.54; 146.04; 146.11; 146.44; 146.48; 147.23; 147.27; 163.23; 163.44; 163.53; 167.68; 168.44. MALDI-TOF-MS (CCA): 1601 (M^-; calc. for $^{13}C^{12}C_{107}H_{48}O_{16}$: 1601). HR-FAB-MS: 1600.2931 (M^+, $^{12}C_{108}H_{48}O_{16}^+$; calc. 1600.2942).

Tetraethyl 3'H,3''H-Dicyclopropa[1,9:16,17][5,6]fullerene-C_{60}-I_h-3',3',3'',3''-tetracarboxylate (**9**) [5]. A mixture of **20** (3 mg, 1.87 μmol) and K_2CO_3 (18 mg, 0.130 mmol) in EtOH/THF 1:1 (3.6 ml) was stirred at r.t. under Ar for 4.5 h. After filtration and evaporation, CC (SiO_2, CH_2Cl_2) yielded **9** which was precipitated from its red-brown CH_2Cl_2 soln. by addition of hexane: 1.5 mg, 77%. Brown solid. ^{1}H-NMR (200 MHz, $CDCl_3$): 1.41 (*t*, *J* = 7.1, 3H); 1.44 (*t*, *J* = 7.1, 6H); 1.45 (*t*, *J* = 7.1, 3H); 4.45 (*q*, *J* = 7.1, 2H); 4.49 (*q*, *J* = 7.1, 2H); 4.51 (*q*, *J* = 7.1, 4H). MALDI-TOF-MS (DHB): 1036 (M^-; calc. for $^{12}C_{74}H_{20}O_8$: 1036).

3',3'-Bis{{4-[2-[3,4-bis(methoxycarbonyl)phenyl]ethyl}phenyl}methyl} 3'',3''',3'''',3'''''-Tetrakis(2-ethoxy-2-oxoethyl) 3'H,3''H,3'''H-Tricyclopropa[1,9:16,17:52,60][5,6]fullerene-C_{60}-I_h-3',3',3'',3'',3''',3'''-hexacarboxylate (**23**). A soln. of **5** (120 mg, 0.070 mmol) and C_{60} (59 mg, 0.081 mmol) in PhCl (270 ml) was irradiated in a photoreactor at r.t. for 2 h, while O_2 was bubbled through. The mixture (TLC (SiO_2, CH_2Cl_2/AcOEt 19:1): R_f 0.15) was transferred into a flask and deoxygenated by inserting a stream of Ar, and PPh_3 (184 mg, 0.701 mmol) in PhCl (4 ml) was added. After stirring at r.t. for 3 h under Ar, plug filtration (SiO_2) with PhMe to remove PhCl and C_{60}, then with CH_2Cl_2/AcOEt 9:1 and then 4:1, yielded an orange-red soln., and evaporation and drying gave **22** (106 mg, 86%). MALDI-TOF-MS (CCA): 1743 (100, M^+; calc. for $^{13}C^{12}C_{110}H_{58}O_{22}$: 1743), 1471 (23, $[M-C(CO_2CH_2CO_2Et)_2]^+$), 1201 (8, $[M-2\ C(CO_2CH_2CO_2Et)_2]^+$).

The isomer mixture **22** (105 mg, 0.060 mmol), TsOH (34 mg, 0.180 mmol), and DMAD (85 mg, 0.602 mmol) were heated to reflux in deoxygenated PhMe (125 ml) in the dark for 5 h after which time the soln. became dark-red. CC (SiO_2, PhMe, then CH_2Cl_2, then CH_2Cl_2/AcOEt 19:1 then 9:1) yielded **23** as a brown product, that was precipitated from CH_2Cl_2 by addition of hexane: 58 mg, 48%. Brown solid. M.p. 135° (dec.). UV/VIS (CH_2Cl_2): 621 (580), 573 (sh, 1000), 504 (sh, 2450), 462 (5100), 434 (3700), 403 (sh, 4500), 342 (sh, 26100), 303 (sh, 51800), 281 (sh, 75700), 251 (sh, 118700). IR (KBr): 2944*m*, 2856*m*, 1739*s*, 1600*m*, 1567*w*, 1506*w*, 1428*s*, 1378*s*, 1294*s*, 1189*s*, 1122*s*, 1067*s*, 1022*s*, 844*m*, 817*m*, 789*m*, 736*m*, 706*m*, 675*m*, 583*w*, 555*m*, 533*m*, 524*s*. ^{1}H-NMR (500 MHz, $CDCl_3$): 1.23 (*t*, *J* = 7.1, 3H); 1.26 (*t*, *J* = 7.1, 3H); 1.29 (*t*, *J* = 7.1, 6H); 2.93 (*m*, 8H); 3.88 (*s*, 6H); 3.90 (*s*, 6H); 4.21 (*q*, *J* = 7.1, 2H); 4.24 (*q*, *J* = 7.1, 2H); 4.27 (*q*, *J* = 7.1, 4H); 4.847 (*s*, 2H); 4.848 (*s*, 2H); 4.97 (*d*, *J* = 15.7, 2H); 5.01 (*d*, *J* = 15.7, 2H); 5.40 (*d*, *J* = 12.0, 2H); 5.46 (*d*, *J* = 12.0, 2H); 7.15 (*dm*, *J* = 8.1, 4H); 7.27 (*dd*, *J* = 7.9, 1.7, 2H); 7.35 (*dm*, *J* = 8.1, 4H); 7.50 (*d*, *J* = 1.7, 2H); 7.66 (*d*, *J* = 7.9, 2H). ^{13}C-NMR (125.8 MHz, $CDCl_3$): 14.10; 14.12; 14.16; 36.95; 37.34; 43.57; 44.33; 52.49; 52.62; 61.68; 61.73; 61.74; 62.58; 62.74; 68.56; 68.69; 68.96; 69.43; 69.84; 71.24; 128.63; 128.66; 129.14; 129.26; 129.27; 130.89; 132.57; 132.68; 139.28; 139.95; 140.26; 141.59; 142.20; 142.36; 142.62; 142.76; 142.88; 142.94; 143.46; 143.47; 143.55; 143.62; 143.76; 143.83; 144.24; 144.33; 144.94; 144.97; 145.04; 145.12; 145.15; 145.20; 145.36; 145.93; 145.98; 147.37; 162.51; 162.57; 162.83; 163.62; 166.39; 166.40; 166.45; 167.67; 168.40. MALDI-TOF-MS (CCA): 1991 (100, M^-; calc. for $^{13}C^{12}C_{122}H_{66}O_{28}$: 1991), 1717 (52, $[M-C(CO_2CH_2CO_2Et)_2]^-$). HR-FAB-MS: 1990.3742 (M^+, $^{12}C_{123}H_{66}O_{28}^+$; calc. 1990.3740).

Hexaethyl 3'H,3''H,3'''H-Tricyclopropa[1,9:16,17:52,60][5,6]fullerene-C_{60}-I_h-3',3',3'',3'',3''',3'''-hexacarboxylate (**10**). A mixture of **23** (12 mg, 6.02 μmol) and K_2CO_3 (60 mg, 0.434 mmol) in EtOH/THF 1:1 (12 ml) was stirred at r.t. under Ar for 1.5 h. After plug filtration and evaporation, CC (SiO_2, CH_2Cl_2/hexane 2:1, then CH_2Cl_2) yielded **10** which was precipitated from its red-brown CH_2Cl_2 soln. by addition of hexane: 6 mg, 83%. Brown solid. M.p. > 270°. UV/VIS (CH_2Cl_2): 621 (sh, 250), 501 (sh, 1850), 463 (4400), 436 (2700), 405 (sh, 3000), 342 (sh, 21900), 302 (sh, 43900), 279 (68000), 250 (sh, 95100), 234 (95100). IR (KBr): 2974*m*, 2930*m*, 2868*w*, 1743*s*, 1460*m*, 1445*m*, 1422*w*, 1389*m*, 1366*m*, 1295*m*, 1246*s*, 1212*s*, 1175*m*, 1105*m*, 1094*m*, 1075*m*, 1026*m*, 857*w*, 737*w*, 707*w*, 675*w*, 580*w*, 550*w*, 533*m*, 524*m*. ^{1}H-NMR (500 MHz, $CDCl_3$): 1.37 (*t*, *J* = 7.1, 6H); 1.49 (*t*, *J* = 7.1, 12H); 4.41 (*q*, *J* = 7.1, 4H); 4.56 (*m*, 8H). ^{13}C-NMR (125 MHz, $CDCl_3$): 14.07; 14.24; 44.69; 54.33; 63.08; 63.28; 69.08; 70.03; 71.88; 139.34; 140.58; 142.27; 142.52; 142.83; 143.57; 143.80; 144.12; 144.36; 145.08; 145.14; 145.44; 146.06; 147.29; 163.60; 163.94. FAB-MS: 1195 (100, MH^+), 1194 (90, M^+, $^{12}C_{81}H_{30}O_{12}^+$), 1149 (28, $[M-OCH_2CH_3]^+$), 720 (50, C_{60}^+). HR-FAB-MS: 1194.1725 (M^+, $^{12}C_{81}H_{30}O_{12}^+$; calc. 1194.1737).

Competition Experiment to Evaluate Relative Chemical Reactivities. To a soln. of **11** (8.00 mg, 5.91 μmol) and **4** (7.80 mg, 5.91 μmol) in dry degassed PhCl (100 ml) was added diethyl 2-bromomalonate (5.91 μmol, 63 μl of a soln. prepared by dissolving 800 μl of the malonate in PhCl (50 ml)) and DBU (5.89 μmol, 55 μl of a soln. prepared by dissolving 800 μl of DBU in PhCl (50 μl)), and the mixture was stirred at r.t. for 2 d. Dilution with PhCl, CC (SiO_2-*H*, PhMe, then PhMe/Et_2O 49:1) afforded unreacted **4** (4.09 mg, 3.09 mmol) and **11** (1.52 mg, 1.12 mmol) in a ratio of 2.7:1, in addition to a mixture of pentakis-adducts **5**/**6** and hexakis-adduct **38**.

X-Ray Structure of **11**. The X-ray measurements were made on a *Nonius-CAD4* diffractometer equipped with a graphite monochromator (MoK_α radiation, λ 0.7107 Å) and a *Nonius* gas-stream low-temp. device. Black, plate-like single crystals of **11** were obtained by very slow evaporation of a $CHCl_3$ soln. at r.t. The crystals belong to the triclinic space group $P\bar{1}$, with half a molecule of **11** and one $CHCl_3$ molecule in the asymmetric unit. The structure of **11** undergoes a phase transformation at *ca.* 252 K, the low-temp. phase being triclinic ($P\bar{1}$) as well. The unit-cell parameters of the two phases, obtained *ca.* 3° above the transition temp. and *ca.* 2° below (in parentheses), are a = 10.024(9.989) Å, b = 13.358(13.462) Å, c = 13.875(13.912) Å, α = 78.40(75.56)°, β = 72.13(71.35)°, γ = 73.85(73.35)°, V = 1685(1672) Å^3. The high- and low-temp. structures of **11** were determined at 258 and 100 K, resp. The structures were solved by direct methods and refined by full-matrix least-squares analysis (SHELXTL PLUS). Heavy atoms were refined anisotropically, H-atoms isotropically, whereby H-positions were based on stereochemical considerations. Experimental parameters of the low-temp. analysis are summarized in *Table 3*, and further details are available on request (No. CCDC-10/34) from the Director of the *Cambridge Crystallographic Data Centre*, 12 Union Road, GB-Cambridge CB12 1EZ (UK), on quoting the full journal citation.

Table 3. *Experimental Details of the X-Ray Analysis of* **11** *at 100 K*

Empirical formula	$C_{88}H_{40}O_{16} \cdot 2\ CHCl_3$
Temp. of data collection [K]	100
Crystal dimensions [mm]	*ca.* 0.30 × 0.25 × 0.20
Space group	$P\bar{1}$
Cell dimensions a [Å]	9.894(6)
b [Å]	13.360(4)
c [Å]	13.685(9)
α [°]	75.06(4)
β [°]	71.56(4)
γ [°]	73.65(3)
Formula weight	1591.9
D_c [g cm^{-1}]	1.63
Max. 2 sin θ/λ [Å^{-1}]	1.233
Scan mode	ω/θ
No. of measured reflections	6351
No. of unique reflections	6103
No. of observed reflections ($I > 2\sigma(I)$)	3982
No. of variables in final least-square analysis	527
Type of refinement	F
Exponentially modified weight factor r [Å^2]	5.0
Extinction correction	isotropic
$R(F)$	0.041
$R_w(F)$	0.046

This work was supported by the *Swiss National Science Foundation*. We are grateful to Mr. *Thomas Mäder* for assistance with the HPLC separation, to Mr. *Hans-Ulrich Hediger* for recording the MALDI-TOF mass spectra, and Mr. *Rolf Häfliger* for recording the FAB- and HR-FAB mass spectra.

REFERENCES

[1] L. Isaacs, F. Diederich, R. F. Haldimann, *Helv. Chim. Acta* **1997**, *80*, 317.
[2] a) L. Isaacs, R. F. Haldimann, F. Diederich, *Angew. Chem.* **1994**, *106*, 2434; *ibid. Int. Ed.* **1994**, *33*, 2339; b) L. Isaacs, P. Seiler, F. Diederich, *Angew. Chem.* **1995**, *107*, 1636; *ibid. Int. Ed.* **1995**, *34*, 1466.
[3] C. Boudon, J.-P. Gisselbrecht, M. Gross, L. Isaacs, H. L. Anderson, R. Faust, F. Diederich, *Helv. Chim. Acta* **1995**, *78*, 1334.
[4] F. Cardullo, L. Isaacs, F. Diederich, J.-P. Gisselbrecht, C. Boudon, M. Gross, *Chem. Commun.* **1996**, 797.
[5] A. Hirsch, I. Lamparth, H. R. Karfunkel, *Angew. Chem.* **1994**, *106*, 453; *ibid. Int. Ed.* **1994**, *33*, 437.
[6] a) C. Bingel, *Chem. Ber.* **1993**, *126*, 1957; b) F. Diederich, L. Isaacs, D. Philp, *J. Chem. Soc., Perkin Trans. 2* **1994**, 391.

[7] A. Hirsch, I. Lamparth, T. Grösser, *J. Am. Chem. Soc.* **1994**, *116*, 9385.
[8] J.-F. Nierengarten, A. Herrmann, R. R. Tykwinski, M. Rüttimann, F. Diederich, C. Boudon, J.-P. Gisselbrecht, M. Gross, *Helv. Chim. Acta* **1997**, *80*, 293.
[9] J.-F. Nierengarten, V. Gramlich, F. Cardullo, F. Diederich, *Angew. Chem.* **1996**, *108*, 2242; *ibid. Int. Ed.* **1996**, *35*, 2101.
[10] a) I. Lamparth, C. Maichle-Mössmer, A. Hirsch, *Angew. Chem.* **1995**, *107*, 1755; *ibid. Int. Ed.* **1995**, *34*, 1607; b) I. Lamparth, A. Herzog, A. Hirsch, *Tetrahedron* **1996**, *52*, 5065; c) P. Timmerman, L. E. Witschel, F. Diederich, C. Boudon, J.-P. Gisselbrecht, M. Gross, *Helv. Chim. Acta* **1996**, *79*, 6; d) S. R. Wilson, Q. Lu, *Tetrahedron Lett.* **1995**, *36*, 5707; e) E. Nakamura, H. Isobe, H. Tokuyama, M. Sawamura, *Chem. Commun.* **1996**, 1747.
[11] a) Y. Rubin, S. Khan, D. I. Freedberg, C. Yeretzian, *J. Am. Chem. Soc.* **1993**, *115*, 344; b) P. Belik, A. Gügel, J. Spickermann, K. Müllen, *Angew. Chem.* **1993**, *105*, 95; *ibid. Int. Ed.* **1993**, *32*, 78.
[12] a) B. Kräutler, M. Puchberger, *Helv. Chim. Acta* **1993**, *76*, 1626; b) B. Kräutler, J. Maynollo, *Angew. Chem.* **1995**, *107*, 69; *ibid. Int. Ed.* **1995**, *34*, 87; c) B. Kräutler, T. Müller, J. Maynollo, K. Gruber, C. Kratky, P. Ochsenbein, D. Schwarzenbach, H.-B. Bürgi, *Angew. Chem.* **1996**, *108*, 1294; *ibid. Int. Ed.* **1996**, *35*, 1204.
[13] a) Y.-Z. An, G. A. Ellis, A. L. Viado, Y. Rubin, *J. Org. Chem.* **1995**, *60*, 6353; b) Y.-Z. An, A. L. Viado, M.-J. Arce, Y. Rubin, *ibid.* **1995**, *60*, 8330.
[14] a) J. W. Arbogast, A. P. Darmanyan, C. S. Foote, Y. Rubin, F. Diederich, M. M. Alvarez, S. J. Anz, R. L. Whetten, *J. Phys. Chem.* **1991**, *95*, 11; b) H. Tokuyama, E. Nakamura, *J. Org. Chem.* **1994**, *59*, 1135; c) J. L. Anderson, Y.-Z. An, Y. Rubin, C. S. Foote, *J. Am. Chem. Soc.* **1994**, *116*, 9763; d) M. Orfanopoulos, S. Kambourakis, *Tetrahedron Lett.* **1994**, *35*, 1945.
[15] G. O. Schenck, H. Eggert, W. Denk, *Liebigs Ann. Chem.* **1953**, *584*, 177.
[16] D. Seebach, E. Hungerbühler, R. Naef, P. Schnurrenberger, B. Weidmann, M. Züger, *Synthesis* **1982**, 138.
[17] P. Seiler, L. Isaacs, F. Diederich, *Helv. Chim. Acta* **1996**, *79*, 1047.
[18] H. L. Anderson, C. Boudon, F. Diederich, J.-P. Gisselbrecht, M. Gross, P. Seiler, *Angew. Chem.* **1994**, *106*, 1691; *ibid. Int. Ed.* **1994**, *33*, 1628.
[19] P. Timmerman, H. L. Anderson, R. Faust, J.-F. Nierengarten, T. Habicher, P. Seiler, F. Diederich, *Tetrahedron* **1996**, *52*, 4925.
[20] S. Ravaine, F. Vicentini, M. Mauzac, P. Delhaes, *New J. Chem.* **1995**, *19*, 1.
[21] T. Chuard, R. Deschenaux, *Helv. Chim. Acta* **1996**, *79*, 736; H. Murakami, Y. Watanabe, N. Nakashima, *J. Am. Chem. Soc.* **1996**, *118*, 4484.
[22] a) A. Vasella, P. Uhlmann, C. A. A. Waldraff, F. Diederich, C. Thilgen, *Angew. Chem.* **1992**, *104*, 1383; *ibid. Int. Ed.* **1992**, *31*, 1388; b) L. Isaacs, A. Wehrsig, F. Diederich, *Helv. Chim. Acta* **1993**, *76*, 1231; c) F. Diederich, U. Jonas, V. Gramlich, A. Herrmann, H. Ringsdorf, C. Thilgen, *ibid.* **1993**, *76*, 2445.
[23] P. J. Fagan, J. C. Calabrese, B. Malone, *J. Am. Chem. Soc.* **1991**, *113*, 9408.
[24] A. Hirsch, Habilitationsschrift, Eberhard-Karls-Universität Tübingen, 1994.
[25] a) G. Schick, A. Hirsch, H. Mauser, T. Clark, *Chem. Eur. J.* **1996**, *2*, 935; b) Q. Lu, D. I. Schuster, S. R. Wilson, *J. Org. Chem.* **1996**, *61*, 4764.
[26] a) D. M. Guldi, H. Hungerbühler, K.-D. Asmus, *J. Phys. Chem.* **1995**, *99*, 9380; b) M. Eiermann, R. C. Haddon, B. Knight, Q. C. Li, M. Maggini, N. Martín, T. Ohno, M. Prato, T. Suzuki, F. Wudl, *Angew. Chem.* **1995**, *107*, 1733; *ibid. Int. Ed.* **1995**, *34*, 1591; c) N. Liu, H. Touhara, Y. Morio, D. Komichi, F. Okino, S. Kawasaki, *J. Electrochem. Soc.* **1996**, *143*, L214; d) F. Zhou, G. J. Van Berkel, B. T. Donovan, *J. Am. Chem. Soc.* **1994**, *116*, 5485; e) S. Lerke, B. A. Parkinson, D. H. Evans. P. J. Fagan, *ibid.* **1992**, *114*, 7807.
[27] a) T. Suzuki, Q. Li, K. C. Khemani, F. Wudl, Ö. Almarsson, *J. Am. Chem. Soc.* **1992**, *114*, 7300; b) K. Komatsu, A. Kagayama, Y. Murata, N. Sugita, K. Kobayashi, S. Nagase, T. S. M. Wan, *Chem. Lett.* **1993**, 2163; c) M. Eiermann, F. Wudl, M. Prato, M. Maggini, *J. Am. Chem. Soc.* **1994**, *116*, 8364; d) F. Arias, Q. Xie, Y. Wu, Q. Lu, S. R. Wilson, L. Echegoyen, *ibid.* **1994**, *116*, 6388; e) T. Suzuki, Y. Maruyama, T. Akasaka, W. Ando, K. Kobayashi, S. Nagase, *ibid.* **1994**, *116*, 1359; f) F. Arias, L. Echegoyen, S. R. Wilson, Q. Lu, Q. Lu, *ibid.* **1995**, *117*, 1422; g) J. C. Hummelen, B. W. Knight, F. LePeq, F. Wudl, J. Yao, C. L. Wilkins, *J. Org. Chem.* **1995**, *60*, 532; h) F. Paolucci, M. Marcaccio, S. Roffia, G. Orlandi, F. Zerbetto, M. Prato, M. Maggini, G. Scorrano, *J. Am. Chem. Soc.* **1995**, *117*, 6572; i) M. Fedurco, D. A. Costa, A. L. Balch, W. R. Fawcett, *Angew. Chem.* **1995**, *107*, 220; *ibid. Int. Ed.* **1995**, *34*, 194; j) S. Ravaine, F. Vicentini, M. Mauzac, P. Delhaes, *New J. Chem.* **1995**, *19*, 1; k) K. Komatsu, N. Takimoto, Y. Murata, T. S. M. Wan, T. Wong, *Tetrahedron Lett.* **1996**, *37*, 6153; m) Y. Murata, K. Motoyama, K. Komatsu, T. S. M. Wan, *Tetrahedron* **1996**, *52*, 5077.
[28] D. Bakowies, Doctoral Dissertation, University of Zürich, Zürich, 1994.

[29] M. J. S. Dewar, W. Thiel, *J. Am. Chem. Soc.* **1977**, *99*, 4899.
[30] R. Ahlrichs, M. Bär, M. Häser, H. Horn, C. Kölmel, *Chem. Phys. Lett.* **1989**, *162*, 165; M. Häser, R. Ahlrichs, *J. Comput. Chem.* **1989**, *10*, 104.
[31] S. Patchkovskii, W. Thiel, *Theor. Chim. Acta* **1996**, *93*, 87.
[32] L.-S. Wang, J. Conceicao, C. Jin, R. E. Smalley, *Chem. Phys. Lett.* **1991**, *182*, 5.
[33] A. Hirsch, 'The Chemistry of the Fullerenes', Georg Thieme, Stuttgart, 1994, p. 32; W. Krätschmer, L. D. Lamb, K. Fostiropoulos, D. R. Huffman, *Nature (London)* **1990**, *347*, 354.
[34] Z. C. Wu, D. A. Jelski, T. F. George, *Chem. Phys. Lett.* **1987**, *137*, 291; S. J. Cyvin, E. Brensdal, B. N. Cyvin, J. Brunvoll, *ibid.* **1988**, *143*, 377; R. E. Stanton, M. D. Newton, *J. Phys. Chem.* **1988**, *92*, 2141; D. E. Weeks, W. G. Harter, *J. Chem. Phys.* **1989**, *90*, 4744.
[35] A. Pasquarello, M. Schlüter, R. C. Haddon, *Science (Washington, D.C.)* **1992**, *257*, 1660; A. Pasquarello, M. Schlüter, R. C. Haddon, *Phys. Rev. A* **1993**, *47*, 1783; R. Zanasi, P. W. Fowler, *Chem. Phys. Lett.* **1995**, *238*, 270.
[36] M. Prato, V. Lucchini, M. Maggini, E. Stimpfl, G. Scorrano, M. Eiermann, T. Suzuki, F. Wudl, *J. Am. Chem. Soc.* **1993**, *115*, 8479; M. Prato, T. Suzuki, F. Wudl, V. Lucchini, M. Maggini, *ibid.* **1993**, *115*, 7876.
[37] M. Rüttimann, R. F. Haldimann, L. Isaacs, F. Diederich, A. Khong, H. Jiménez-Vázquez, R. J. Crass, M. Saunders, submitted to *Chem. Eur. J.*
[38] M. Saunders, R. J. Cross, H. A. Jiménez-Vázquez, R. Shimshi, A. Khong, *Science (Washington, D.C.)* **1996**, *271*, 1693.
[39] H. L. Anderson, R. Faust, Y. Rubin, F. Diederich, *Angew. Chem.* **1994**, *106*, 1427; *ibid. Int. Ed.* **1994**, *33*, 1366.
[40] R. F. Haldimann, F.-G. Klärner, F. Diederich, *Chem. Commun.*, in press.
[41] P. Seiler, *Helv. Chim. Acta* **1990**, *73*, 1574.
[42] K. B. Wiberg, W. P. Dailey, F. H. Walker, S. T. Waddell, L. S. Crocker, M. Newton, *J. Am. Chem. Soc.* **1985**, *107*, 7247.